Diabetologia (2010) 53:1727–1731
DOI 10.1007/s00125-010-1744-6

SHORT COMMUNICATION

Angiotensin II type 1 receptor-independent beneficial effects of telmisartan on dietary-induced obesity, insulin resistance and fatty liver in mice

X. Rong · Y. Li · K. Ebihara · M. Zhao · J. Naowaboot · T. Kusakabe · K. Kuwahara · M. Murray · K. Nakao

Received: 4 January 2010 / Accepted: 4 March 2010 / Published online: 15 April 2010

Abstract
Aims/hypothesis Evidence suggests that telmisartan, an angiotensin II type 1 receptor (AT1) blocker and peroxisome proliferator-activated receptor-γ partial agonist, has beneficial actions that limit development of the metabolic syndrome and diabetes. However, the role played by AT1 inhibition in metabolic effects elicited by telmisartan remains uncertain. Here we isolated the metabolic effects of telmisartan from AT1 antagonism.
Methods Male *At1a* (also known as *Agtr1a*)-deficient mice were fed a standard diet or 60% high-fat diet; those on high-fat diet were co-administered telmisartan (3 mg kg^{-1} day^{-1} by oral gavage) or vehicle for 12 weeks.
Results In *At1a*-null mice, telmisartan prevented high-fat-diet-induced increases in (1) body weight, epididymal and inguinal white adipose tissue weight, adipocyte size and plasma leptin concentration; (2) plasma glucose and insulin concentrations and HOMA index; and (3) liver weight and triacylglycerol content. Insulin tolerance testing also indicated that telmisartan improved the high-fat-diet-induced reduction of glucose-lowering by insulin.
Conclusions/interpretation The present findings demonstrate beneficial, AT1-independent effects of the AT1 blocker telmisartan on dietary-induced obesity, insulin resistance and fatty liver in animals.

Keywords Angiotensin II type 1 receptor · Fatty liver · Insulin resistance · Obesity · Telmisartan

Abbreviations

ARB	Angiotensin II type 1 receptor blocker
AT1	Angiotensin II type 1 receptor
eWAT	Epididymal white adipose tissue
HFD	High-fat diet
ITT	Insulin tolerance test
iWAT	Inguinal white adipose tissue
KO	Knockout
PPAR	Peroxisome proliferator-activated receptor

Introduction

The metabolic syndrome is a cluster of conditions arising from overnutrition and a sedentary lifestyle. Common components of the metabolic syndrome include abdominal obesity, insulin resistance, hypertension and dyslipidaemia. Additional comorbidities may also be present, such as hepatic steatosis leading to non-alcoholic fatty liver disease, proinflammatory and prothrombotic states, and reproductive disorders [1]. Insulin resistance is the key component of the metabolic syndrome. It precedes and predicts the incidence and development of type 2 diabetes and cardiovascular diseases [2].

It has been suggested that activation of the renin–angiotensin system is a common feature in patients with

Electronic supplementary material The online version of this article (doi:10.1007/s00125-010-1744-6) contains supplementary material, which is available to authorised users.

X. Rong · Y. Li (✉) · K. Ebihara · M. Zhao · J. Naowaboot · T. Kusakabe · K. Kuwahara · K. Nakao
Department of Medicine and Clinical Science,
Kyoto University Graduate School of Medicine,
Kyoto 606-8507, Japan
e-mail: yuhao@kuhp.kyoto-u.ac.jp

M. Murray
Laboratory of Pharmacogenomics, Faculty of Pharmacy,
The University of Sydney,
Sydney, NSW 2006, Australia

obesity/the metabolic syndrome [2]. Indeed, blockade of the renin–angiotensin system has been shown in clinical and experimental studies to improve the metabolic syndrome [2]. Most of the established physiological and pathophysiological effects of angiotensin II appear to be mediated through the angiotensin II type 1 receptor (AT1). Angiotensin II type 1 receptor blockers (ARBs) have been used widely in the clinic as antihypertensive agents. More recently, treatment with some ARBs has been found to improve insulin resistance and to protect against the onset and development of type 2 diabetes in insulin-resistant patients with hypertension [2]. Studies in experimental animals seem to support clinical findings [2]. Thus, although the precise mechanisms have yet to be established, the contribution of AT1 signalling and the beneficial effects of AT1 inhibition in the metabolic syndrome are undoubted.

Telmisartan is a well-established ARB. Recently, it was shown to be a partial agonist of the peroxisome proliferator-activated receptor (PPAR)γ in cultured cells [3, 4] and to activate PPARα in cultured hepatic cells and in liver of wild-type mice fed a high-fat diet (HFD) [5]. Telmisartan has also been reported to improve HFD-induced obesity, insulin resistance and fatty liver in wild-type animals [4, 5]. However, the extent to which AT1 inhibition contributes to the beneficial effects of telmisartan treatment has not yet been established. The present study tests the role of AT1 inhibition in telmisartan-elicited metabolic effects using HFD-fed *Atl1a* (also known as *Agtr1a*)-knockout (KO) mice.

Methods

Animals, diet and experimental protocol All animal procedures were in accordance with the Principles of Laboratory Animal Care (http://grants1.nih.gov/grants/olaw/references/phspol.htm) and were approved by the Animal Ethics Committee, Kyoto University, Japan. Mice were housed in a temperature-controlled facility (21±1°C, 55±5% relative humidity) with a 12-h light/dark cycle (three to four mice per cage).

Male C57BL/6J wild-type mice were purchased from Japan SLC (Shizuoka, Japan). Male *Atl1a*-KO mice on a C57BL/6J background were generated by methods that have been described previously [6]. Animals (8 weeks of age) were divided into three groups (n=8–10 each): (1) standard diet control (standard diet Tel−); (2) HFD control (HFD Tel−); and (3) HFD telmisartan (HFD Tel+) groups. The animals had free access to water and the standard diet (CLEA, Tokyo, Japan) (Tel− group) or HFD (containing 20% [wt/wt] protein, 20% [wt/wt] carbohydrate and 60% [wt/wt] fat) (D12492; Research Diet, New Brunswick, NJ, USA) (HFD Tel− and HFD Tel+ groups). Animals receiving the HFD were also administered telmisartan (3 mg/kg suspended in 5% (wt/vol.) gum arabic (a gift from Boehringer Ingelheim, Tokyo, Japan) or vehicle by oral gavage once daily (between 11:00 and 12:00 hours) for 12 weeks. Daily (24 h) food intake was estimated from weekly measurements. Systolic BP was measured by a tail-cuff method (MK-2000ST; Muromachi Kikai, Tokyo, Japan) at week 5. Blood samples were collected by retroorbital venous puncture under ether anaesthesia at week 10 in animals in non-fasted and fasted (12 h) states. Insulin tolerance tests (ITT; 0.75 IU/kg, i.p.; Humulin R-Insulin; Eli Lilly, Indianapolis, IN, USA) were conducted after fasting (6 h) at week 11. After animals were weighed at week 12, blood samples were collected again from non-fasted animals. Immediately thereafter animals were killed by prompt dislocation of the neck vertebra. Epididymal white adipose tissue (eWAT), inguinal white adipose tissue (iWAT) and liver were collected and weighed. Gastrocnemius was also collected. Glucose, triacylglycerol and NEFA concentrations were determined colorimetrically (Wako, Osaka, Japan), and insulin and leptin concentrations were analysed by ELISA (Morinaga, Tokyo, Japan). HOMA was calculated by method that has been described previously [7].

A portion of eWAT or liver was fixed with 10% formalin (vol./vol.) and embedded in paraffin. Sections (20 μm) were cut and stained with haematoxylin and eosin for examination of adipose tissue and liver histology (IX-81; Olympus, Tokyo, Japan). The adipocyte cross-sectional area was measured using an image analysing system (KS 400; Carl Zeiss Vision, Eching, Germany).

Data analysis All results are expressed as means ± SEM. Data were analysed by one-way ANOVA. If a difference was detected (F ratio), the Student–Newman–Keuls test was performed to locate the differences between groups. Values of $p<0.05$ were considered to be statistically significant.

Results

Consistent with previous reports [4, 5], we have demonstrated that telmisartan treatment (3 mg/kg) did not affect food intake (Electronic supplementary material [ESM] Fig. 1b), but substantially attenuated HFD-induced obesity (ESM Fig. 1c–h), insulin resistance (ESM Fig. 2a–e) and lipid overaccumulation in liver and skeletal muscle (ESM Fig. 3c–g) in C57BL/6J wild-type mice. In the present study, systolic BP in *Atl1a*-KO mice was 75±2.5 mmHg (Fig. 1a), which was lower than in wild-type mice (ESM Fig. 1a); telmisartan did not alter systolic BP in *Atl1a*-KO mice.

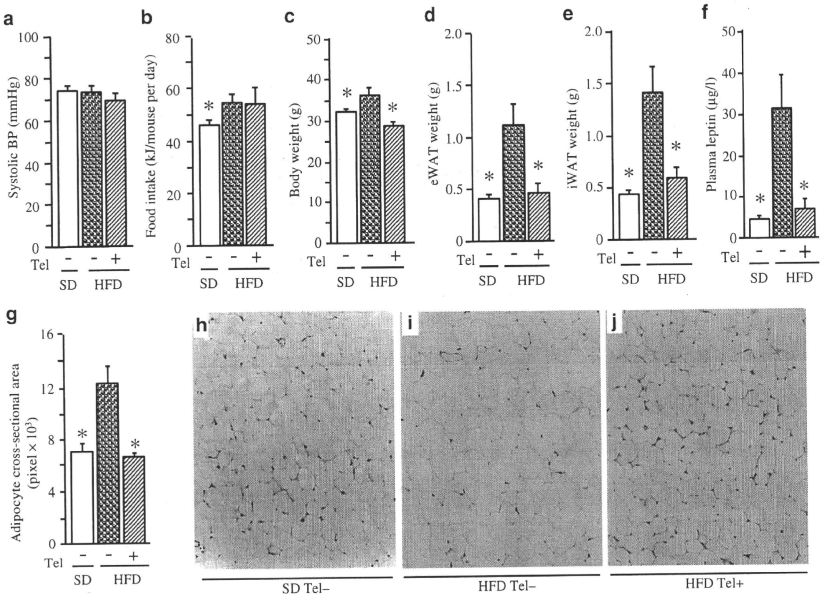

Fig. 1 Systolic BP (**a**), food intake per day (**b**), body weight (**c**), eWAT weight (**d**), iWAT weight (**e**), plasma leptin concentration (**f**), adipocyte cross-sectional area (**g**) and representative images (**h–j**) showing histology of eWAT (haematoxylin and eosin staining, magnification ×200) in male *Atl1*-KO mice fed standard or HFD for 12 weeks. All values are means ± SEM (n=8–10); *p<0.05 vs HFD control (Tel–). Tel–, vehicle; Tel+, telmisartan 3 mg/kg

HFD feeding significantly increased food intake (Fig. 1b), body weight (Fig. 1c), the weight of eWAT (Fig. 1d) and iWAT (Fig. 1e), adipocyte size (Fig. 1g–i) and plasma leptin concentration (Fig. 1f) in *Atl1*-KO mice. Telmisartan treatment did not affect food intake, but did ameliorate other variables (Fig. 1c–g, j).

In *Atl1*-KO mice, HFD feeding increased the fasted plasma glucose (Fig. 2a) and insulin (Fig. 2b) concentrations, and the HOMA index (Fig. 2c) in comparison with those in standard diet-fed *Atl1*-KO mice. Plasma glucose concentrations after insulin challenge (Fig. 2d) and the glucose AUC during ITT (Fig. 2e) were also increased by HFD treatment. Telmisartan treatment suppressed the HFD-induced increase in all variables.

HFD feeding had no effect on non-fasted and fasted plasma concentrations of triacylglycerol and NEFA (Fig. 2f, g), and on liver weight (Fig. 2h), whereas triacylglycerol content in liver and skeletal muscle was increased against that in standard diet-fed *Atl1*-KO mice (Fig. 2i, j). Telmisartan treatment decreased liver weight and triacylglycerol content in liver and skeletal muscle. Histological evaluation confirmed that fatty infiltration of the liver was decreased by telmisartan (data not shown). In contrast with the lipid-lowering effects observed in HFD-fed wild-type rats [4] and mice (ESM Fig. 3a, b), telmisartan minimally affected non-fasted and fasted plasma triacylglycerol and NEFA concentrations in HFD-fed *Atl1*-KO mice.

Discussion

The present study demonstrates that long-term treatment with telmisartan in *Atl1*-null mice fed a HFD prevents or improves the increase in: (1) body weight, white adipose tissue weight, adipocyte size and plasma leptin concentration; (2) plasma glucose and insulin concentrations, HOMA index, and plasma glucose concentrations and glucose AUC during ITT; and (3) liver weight and triacylglycerol content of the

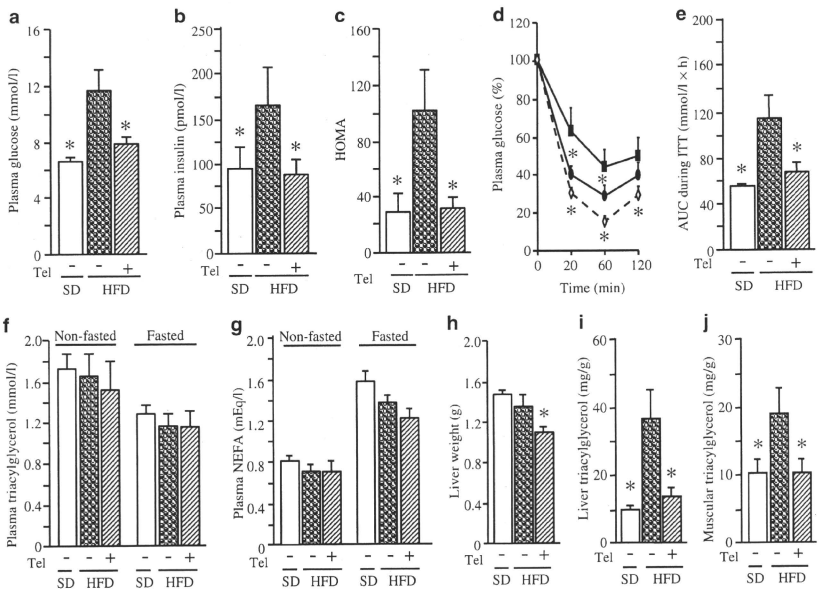

Fig. 2 Fasted (12 h) plasma concentrations of glucose (**a**) and insulin (**b**), HOMA index (**c**), plasma glucose response curve (per cent glucose change) (**d**), plasma glucose AUC following insulin challenge in ITT (Insulin 0.75 IU/kg, i.p.) (**e**), non-fasted and fasted plasma triacylglycerol concentrations (**f**), NEFA concentrations (**g**), liver weight (**h**), and triacylglycerol content of liver and skeletal muscle respectively (**i**, **j**) in male *Atl a*-KO mice fed a standard diet or HFD. All values are means ± SEM (n=8–10); *p<0.05 vs HFD control (Tel−). Tel−, vehicle; Tel+, telmisartan 3 mg/kg; (**d**) white diamonds, standard diet Tel−; black squares, HFD Tel−; black ovals, HFD Tel+

liver and skeletal muscle. The present findings reveal AT1-independent improvement of dietary-induced obesity, insulin resistance and fatty liver following telmisartan treatment.

Obesity is a well-established metabolic and cardiovascular risk factor. Recent advances have increased our understanding of the cellular mechanisms whereby adiposity induces adverse local and systemic effects. These include lipid accumulation in adipocytes, induction of endoplasmic reticulum and mitochondrial stress, and insulin resistance. Increased adipose tissue mass, especially in the visceral compartment, represents one of the major risk factors for development of type 2 diabetes [8]. We have recently demonstrated that telmisartan treatment improved insulin resistance and fatty liver in A-ZIP/F-1 transgenic mice lacking adipose tissue [7]. These results suggest that telmisartan may elicit its metabolic effects independently of adipose tissue. In the present study, telmisartan treatment attenuated obesity induced by HFD, a finding accompanied by improvement of insulin resistance in wild-type and *Atl a*-KO mice. Thus, the present results suggest that adipose tissue may be an alternative pathway for the insulin-sensitising effect of telmisartan.

On the other hand, an increasing body of evidence indicates that several manifestations of the metabolic syndrome and type 2 diabetes mellitus, including insulin resistance, occur as a result of overaccumulation of lipids in non-adipose tissues, such as liver and skeletal muscle [9]. A decrease in hepatic triacylglycerol pools leads to improved insulin sensitivity [10]. In the present study, HFD-feeding induced excessive lipid accumulation in liver and skeletal muscle, whereas telmisartan treatment ameliorated hepatic steatosis and muscular triacylglycerol deposition in *Atl a*-deficient mice. These results imply that attenuation of diet-induced fatty liver by telmisartan is driven by mechanisms that are independent of AT1. Thus, amelioration of lipid overaccumulation in non-adipose tissues may be an important factor associated with improved insulin action in *Atl a*-null mice following treatment with telmisartan.

In conclusion, the present findings demonstrate for the first time AT1-independent beneficial effects of telmisartan on diet-induced obesity, insulin resistance and fatty liver in mice. Activation of PPARγ might be one potential AT1-independent mechanism of action.

Acknowledgements We thank Y. Yamamoto (Kyoto University) for useful discussions during the preparation of this manuscript and W. Aini for his technical assistance during the project.

Duality of interest The authors declare that there is no duality of interest associated with this manuscript.

References

1. Cornier MA, Dabelea D, Hernandez TL et al (2008) The metabolic syndrome. Endocr Rev 29:777–822
2. Prasad A, Quyyumi AA (2004) Renin–angiotensin system and angiotensin receptor blockers in the metabolic syndrome. Circulation 110:1507–1512
3. Fujimoto M, Masuzaki H, Tanaka T et al (2004) An angiotensin II AT1 receptor antagonist, telmisartan augments glucose uptake and GLUT4 protein expression in 3T3-L1 adipocytes. FEBS Lett 576:492–497
4. Benson SC, Pershadsingh HA, Ho CI et al (2004) Identification of telmisartan as a unique angiotensin II receptor antagonist with selective PPARgamma-modulating activity. Hypertension 43:993–1002
5. Clemenz M, Frost N, Schupp M et al (2008) Liver-specific peroxisome proliferator-activated receptor alpha target gene regulation by the angiotensin type 1 receptor blocker telmisartan. Diabetes 57:1405–1413
6. Li Y, Kishimoto I, Saito Y et al (2002) Guanylyl cyclase-A inhibits angiotensin II type 1A receptor-mediated cardiac remodeling, an endogenous protective mechanism in the heart. Circulation 106:1722–1728
7. Rong X, Li Y, Ebihara K et al (2009) An adipose tissue-independent insulin-sensitizing action of telmisartan: a study in lipodystrophic mice. J Pharmacol Exp Ther 331:1096–1103
8. Bloomgarden ZT (2000) Obesity and diabetes. Diabetes Care 23:1584–1590
9. Unger RH (2002) Lipotoxic diseases. Annu Rev Med 53:319–336
10. Neschen S, Morino K, Hammond LE et al (2005) Prevention of hepatic steatosis and hepatic insulin resistance in mitochondrial acyl-CoA:glycerol-sn-3-phosphate acyltransferase 1 knockout mice. Cell Metab 2:55–65

Am J Physiol Endocrinol Metab 297: E802–E811, 2009.
First published July 14, 2009; doi:10.1152/ajpendo.00205.2009.

A mouse model of ghrelinoma exhibited activated growth hormone-insulin-like growth factor I axis and glucose intolerance

Hiroshi Iwakura,[1] Hiroyuki Ariyasu,[1] Yushu Li,[1] Naotetsu Kanamoto,[2] Mika Bando,[1] Go Yamada,[2] Hiroshi Hosoda,[4] Kiminori Hosoda,[2] Akira Shimatsu,[3] Kazuwa Nakao,[2] Kenji Kangawa,[1,4] and Takashi Akamizu[1]

[1]*Ghrelin Research Project, Translational Research Center, Kyoto University Hospital, Kyoto University Graduate School of Medicine;* [2]*Department of Medicine and Clinical Science, Endocrinology, and Metabolism, Kyoto University Graduate School of Medicine;* [3]*Clinical Research Institute for Endocrine Metabolic Diseases, National Hospital Organization, Kyoto Medical Center, Kyoto; and* [4]*Department of Biochemistry, National Cardiovascular Center Research Institute, Osaka, Japan*

Submitted 27 March 2009; accepted in final form 13 July 2009

Iwakura H, Ariyasu H, Li Y, Kanamoto N, Bando M, Yamada G, Hosoda H, Hosoda K, Shimatsu A, Nakao K, Kangawa K, Akamizu T. A mouse model of ghrelinoma exhibited activated growth hormone-insulin-like growth factor I axis and glucose intolerance. *Am J Physiol Endocrinol Metab* 297: E802–E811, 2009. First published July 14, 2009; doi:10.1152/ajpendo.00205.2009.—Ghrelin is a stomach-derived peptide that has growth hormone-stimulating and orexigenic activities. Although there have been several reports of ghrelinoma cases, only a few cases have elevated circulating ghrelin levels, hampering the investigation of pathophysiological features of ghrelinoma and chronic effects of ghrelin excess. Furthermore, standard transgenic technique has resulted in desacyl ghrelin production only because of the limited tissue expression of ghrelin *O*-acyltransferase, which mediates acylation of ghrelin. Accordingly, we attempted to create ghrelin promoter SV40 T-antigen transgenic (GP-Tag Tg) mice, in which ghrelin-producing cells continued to proliferate and finally developed into ghrelinoma. Adult GP-Tag Tg mice showed elevated plasma ghrelin levels with preserved physiological regulation. Adult GP-Tag Tg mice with increased plasma ghrelin levels exhibited elevated IGF-I levels despite poor nutrition. Although basal growth hormone levels were not changed, those after growth hormone-releasing hormone injection tended to be higher. These results indicate that chronic elevation of ghrelin activates GH-IGF-I axis. In addition, GP-Tag Tg mice demonstrated glucose intolerance. Insulin secretion by glucose tolerance tests was significantly attenuated in GP-Tag Tg, whereas insulin sensitivity determined by insulin tolerance tests was preserved, indicating that chronic elevation of ghrelin suppresses insulin secretion and leads to glucose intorelance. Thus, we successfully generated a Tg model of ghrelinoma, which is a good tool to investigate chronic effects of ghrelin excess. Moreover, their characteristic features could be a hint on ghrelinoma.

ghrelin; glucose metabolism

GHRELIN is a stomach-derived 28-amino acid (AA) peptide hormone with octanoyl modification of third Ser residue, which is essential for its binding to growth hormone (GH) secretagogue receptor (GHS-R) (20). There have been several reports regarding ghrelin-producing tumors (9, 17, 36, 37). As far as we know, only two cases have elevated plasma ghrelin level (9, 36). However, the ghrelin-producing cells in the stomach, known as X/A-like cells, account for about 20% of the endocrine cell population in the oxyntic glands (10). It may be reasonable to estimate that far more ghrelinoma cases have been overlooked and diagnosed as nonfunctioning tumors. Hormone-producing tumors demonstrate their characteristic symptoms by chronic effects of each hormone, which may be a key symptom to making a correct diagnosis. Conversely, the characteristic symptom often tells us the chronic effects of each responsible hormone. Acute effects of ghrelin have been studied extensively by many researchers, and a wide variety of acute effects of ghrelin have been discovered, such as the regulation of growth hormone (GH) release, food intake, gastric acid secretion, gastric motility, blood pressure, and cardiac output (23, 25, 26, 31, 33, 34). However, chronic effects of ghrelin have not been fully understood.

To understand the chronic effects of ghrelin, genetically engineered mouse models would be useful. Several groups, including ours, have developed transgenic animals in which ghrelin transgenes are driven by several different promoters (2, 4, 18, 29, 38, 41). All of these animals except for one line created by Reed et al. (29) using the neuron-specific enolase (NSE) promoter and another line recently reported by Bewick et al. (5) using the bacterial artificial chromosome produced only desacyl ghrelin rather than acylated ghrelin. Until the recent identification of ghrelin *O*-acyltransferase (GOAT), which mediates ghrelin octanoylation (40), it had been unclear how acylation of ghrelin takes place. GOAT is expressed mainly in stomach and intestine, and a small amount of GOAT is also present in pancreas (12). This limited expression area of GOAT made it impossible to create ghrelin-overproducing transgenic animals by standard procedures. When we started this study, GOAT had not yet been identified. Accordingly, we choose an approach in which an increase in the number of ghrelin-producing cells in mice would result in increased levels of circulating ghrelin. By taking this approach, we successfully obtained ghrelin promoter-SV40 T-antigen transgenic (GP-Tag Tg) mice. In these mice, ghrelin concentration elevates with age in concordance with the proliferation of ghrelin cells. The aim of this study was to elucidate the pathophysiological features of ghrelinoma and the chronic effects of ghrelin elevation.

MATERIALS AND METHODS

Animals. Two types of fusion genes comprising the 5′-flanking region of human ghrelin gene (4,085 or 1,479 bp) (19) and SV40 T-antigen were designed (Fig. 1*A*). The purified fragments (10 μg/ml) were microinjected into the pronucleus of fertilized C57/B6 mouse (SLC, Shizuoka, Japan) eggs. The viable eggs were transferred into the oviducts of pseudopregnant female ICR mice (SLC) by using standard techniques. Transgenic founder mice were identified by

Address for reprint requests and other correspondence: H. Iwakura, Ghrelin Research Project, Translational Research Center, Kyoto University Hospital, 54 Shogoin Kawahara-cho, Sakyo-ku, Kyoto 606-8507, Japan (e-mail: hiwaku@kuhp.kyoto-u.ac.jp).

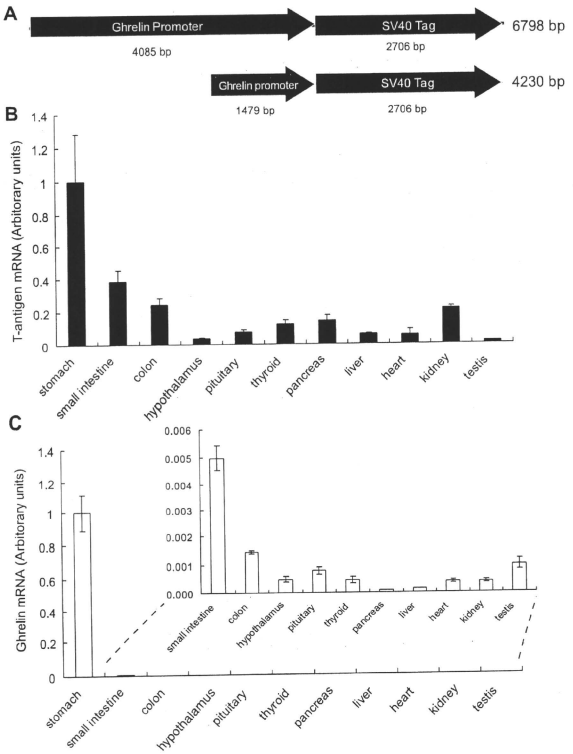

Fig. 1. Constructs of ghrelin promoter-SV40 T-antigen transgenic (GP-Tag Tg) mice and the expression levels of SV40 T-antigen mRNA in various tissues. *A*: 2 types of fusion genes comprising 5′-flanking region of human ghrelin gene (4,085 or 1,479 bp) and SV40 Tag were designed. *B*: the expression levels of SV40 T-antigen mRNA in various tissues of GP-Tag Tg mice at 6 wk of age (n = 8). SV40 T-antigen mRNA was most abundant in the stomachs of GP-Tag Tg mice. *C*: the expression levels of ghrelin mRNA in various tissues of nontransgenic littermates at 6 wk of age (n = 4).

Southern blot analysis of tail DNAs. Transgenic mice were used as heterozygotes. Animals were maintained on standard rodent food (CE-2, 352 kcal/100 g; Japan CLEA, Tokyo, Japan) on a 12:12-h light-dark cycle unless otherwise indicated. All experimental procedures were approved by the Kyoto University Graduate School of Medicine Committee on Animal Research.

RT-PCR and real-time quantitative RT-PCR. Total RNA was extracted using a Sepasol RNA kit (Nacalai Tesque, Kyoto, Japan). Reverse transcription was performed with a high-capacity cDNA reverse transcription kit (Applied Biosystems, Foster City, CA). RT-PCR was carried out with a GeneAmp 9700 using primers in Table 1 with AmpliTaq Gold PCR master mix (Applied Biosystems). Real-time quantitative PCR was performed using an ABI PRISM 7500 Sequence Detection System (Applied Biosystems) with primers and TaqMan probes or with Power SybrGreen (presented in Table 1). The mRNA expression in each gene was normalized to levels of 18S ribosomal RNA.

Immunohistochemistry. Formalin-fixed, paraffin-embedded tissue sections were immunostained using the avidin-biotin peroxidase complex method (Vectastain "ABC" Elite kit; Vector Laboratories, Burlingame, CA), as described previously (18). Sections were incubated with anti-COOH-terminal ghrelin (AA 13-28) (1:2,000 at final dilution), anti-NH_2-terminal ghrelin (14) that recognizes the n-octanoylated portion of ghrelin (AA 1-11) (1:5,000), anti-glucagon (1:500; DAKO, Glostrup, Denmark), anti-somatostatin (1:500; DAKO), anti-gastrin (1:500; DAKO), and anti-GH (1:500; DAKO). The cell number of ghrelin-immunopositive cells was analyzed by WinRoof visual analysis software (Mitani, Fukui, Japan).

Measurements of plasma and tissue ghrelin concentrations. Collection of plasma samples was performed as reported previously (18). Plasma ghrelin and desacyl ghrelin concentrations were determined using two separate ELISA kits, an active ghrelin ELISA kit that recognizes n-octanoylated ghrelin and a desacyl ghrelin ELISA kit (both from Mitsubishi Kagaku Iatron, Tokyo, Japan) (1). Tissue ghrelin concentration was determined by radioimmunoassay (RIA) using anti-ghrelin (AA 13-28) antiserum (C-RIA) and anti-ghrelin (AA 1-11) antiserum (N-RIA), as described previously (18).

Western blot. Stomachs were boiled for 5 min in the 10-fold vol/wt of water. Acetic acid was added to each solution so that the final concentration was adjusted to 1 M, and the tissues were homogenized.

Table 1. *PCR primers and TaqMan probes*

Gene	Primer Sequence
Ghrelin	
Sense	5′-GCATGCTCTGGATGGACATG-3′
Antisense	5′-TGGTGGCTTCTTGGATTCGT-3′
TaqMan probe	5′-AGCCCAGAGCACCAGAAAGCCA-3′
NPY	
Sense	5′-TCCGCTCTGCGACACTACAT-3′
Antisense	5′-GGAAGGGTCTTCAAGCCTTGT-3′
TaqMan probe	5′-CAAGGGCTGGATCTCTTGCCATATCTCTG-3′
AgRP	
Sense	5′-GCTCCACTGAAGGGCATCA-3′
Antisense	5′-TAGCACCTCCGCCAAAGCT-3′
TaqMan probe	5′-TTCCCAGGTCTAAGTCTGAATGGCCTCA-3′
GHRH	
Sense	5′-AGGATGCAGCGACACGTAGA-3′
Antisense	5′-TCTCCCCTTGCTTGTTCATGA-3′
TaqMan probe	5′-CCACCAACTACAGGAAACTCCTGAGCCA-3′
Somatostatin	
Sense	5′-AGCTGAGCAGGACGAGATGAG-3′
Antisense	5′-ACAGGATGTGAATGTCTTCCAGTT-3′
TaqMan probe	5′-CGAACCCAGCAATGGCACCCC-3′
GHS-R	
Sense	5′-CACCAACCTCTACCTATCCAGCAT-3′
Antisense	5′-CTGACAAACTGGAAGAGTTTGCA-3′
TaqMan probe	5′-TCCGATCTGCTCATCTTCCTGTGCATG-3′
GH	
Sense	5′-AAGAGTTCGAGCGTGCCTACA-3′
Antisense	5′-GAAGCAATTCCATGTCGGTTC-3′
TaqMan probe	5′-CCATTCAGAATGCCCAGGCTGCTTTC-3′
GHRH-R	
Sense	5′-GCCCTTGGAACTGTTAACCA-3′
Antisense	5′-GCAACCAGGATGGCAATAGC-3′
TaqMan probe	5′-AGCATCTCCATTGTAGCCCTCTGCGTG-3′
SV40 Tag	
Sense	5′-AAACACTGCAGGCCAGATTT-3′
Antisense with power SYBR Green	5′-AAATGAGCCTTGGGACTGTG-3′
PC1/3	
Sense	5′-AGTGGAAAAGATGGTGAATG-3′
Antisense	5′-CTCCTCATTTAGGATGTCCA-3′

NPY, neuropeptide Y; AgRP, agouti-related protein; GHRH, growth hormone (GH)-releasing hormone; GHS-R, GH secretagogue receptor; GHRH-R, GHRH receptor; PC1/3, prohormone convertase 1/3.

The supernatant was loaded onto a Sep-Pak C18 cartridge (Waters, Milford, MA) preequilibrated with 0.9% NaCl after centrifugation. The cartridge was washed with 2.5 ml of 5% CH_3CN-0.1% trifluoroacetic acid and eluted with 2.5 ml 60% CH_3CN-0.1% trifluoroacetic acid. The eluate was evaporated, lyophilized, and dissolved in Novex Tricine SDS Sample Buffer (Invitrogen, Carlsbad, CA). After being heated at 85°C for 2 min, 20 mg of samples of initial weight were subjected to tricine-SDS PAGE and electroblotted to polyvinylidene fluoride membranes (Invitrogen). Transferred membranes were blocked with Immunoblock (Dainippon Seiyaku, Osaka, Japan) and then incubated with anti-COOH-terminal ghrelin antibody (1:5,000). After being washed with PBS-0.1% Tween-20, membranes were reacted with secondary antibodies and developed with ECL plus (GE Healthcare, Buckinghamshire, UK) as instructed by the manufacturer. The signal on the blot was detected with Lumino-Image Analyzer LAS-3000 mini system (Fuji Photo Film, Tokyo, Japan).

Measurement of food intake. Mice were housed individually with continuous access to chow and water. Food intakes were measured by subtracting the remaining weight of the chow from that originally presented. As for measuring the food intake by ghrelin, ad libitum-fed mice were injected with ghrelin (120 or 360 μg/kg) or saline subcutaneously. Food intakes were measured for 2 h after injection.

Measurements of lean body mass, fat mass, and bone mass. Mice were anesthetized with pentobarbital sodium. Lean body mass, fat mass, and bone mass of mice were measured by an animal computed tomography system (Latheta LTC-100; Aloka, Tokyo, Japan).

Measurements of hormones and blood glucose levels. Serum GH levels were determined by a rat GH EIA kit (SPI Bio, Massy Cedex, France). Serum insulin-like growth factor I (IGF-I) levels were measured using a mouse IGF-I immunoassay kit (R & D Systems, Minneapolis, MN). Blood glucose levels were determined by glucose oxidase method using Glutest Sensor Neo (Sanwa Kagaku, Kyoto, Japan). Measurement of serum insulin concentrations was performed by ELISA using an ultrasensitive rat insulin kit (Morinaga, Yokohama, Japan).

GH-provocative test. GH-provocative test was carried out as described previously (16). Serum samples were collected at 15 min after subcutaneous injection of 180 μg/kg of GH-releasing hormone (GHRH) or 120 μg/kg of ghrelin. We choose these doses according to the results of our previous study (16).

Glucose and insulin tolerance tests. For the glucose tolerance test, after overnight fast, the mice were injected with 1.5 g/kg glucose intraperitoneally. For the insulin tolerance test, after a 4-h fast, mice were injected with 1.0 mU/g human regular insulin (Novolin R; Novo Nordisk, Bagsvaerd, Denmark) intraperitoneally. Blood was sampled from the tail vein before and 30, 60, 90, and 120 min after the injection.

Insulin release. After overnight fast, the mice were injected with 3.0 g/kg glucose intraperitoneally. Blood was sampled from the retroorbital vein at 2 and 30 min after the injection using a glass tube.

Statistical analysis. All values were expressed as means ± SE. The statistical significance of the differences in mean values was assessed by repeated-measures ANOVA or Student's *t*-test. The statistical difference in the changes of plasma ghrelin levels by feeding were assessed by paired *t*-test. Pearson's correlation coefficient analysis and simple regression were used to assess the relations between plasma ghrelin level and body weight. Difference of correlation coefficients of the regression lines obtained from GP-Tag Tg mice and nontransgenic littermates was determined by testing the *t* value.

RESULTS

Generation of GP-Tag Tg mice. By injecting transgenes into 846 eggs, we obtained 11 lines of GP (4.85) Tag Tg mouse. We succeeded in breeding three of these lines (1-5, 3-1, and 4-3). Among these three lines, mice of the 3-1 line developed gastric tumor and showed elevated plasma ghrelin levels, as described below. Mice of the 1-5 line showed very aggressive tumor development and died at ~13 wk of age because of thyroid, pancreatic, and gastric tumors. Mice of the 4-3 line showed very slow tumor development. The proliferation of ghrelin cells was

Fig. 2. Pathological findings and tissue ghrelin concentrations of stomachs in GP-Tag Tg mice. *A–C*: macro findings of stomachs in GP-Tag Tg mice (*A*: arrow, dotted area; *B*: Tg) and nontransgenic littermates (non; *B*) at 12 wk of age. Stomach walls of GP-Tag Tg mice were hypertrophic. *C*: immunohistochemical analysis of ghrelin peptide expression in tissue sections of stomachs of GP-Tag Tg mice (Tg) and nontransgenic littermates (non) using anti-COOH-terminal and anti-NH_2-terminal ghrelin antibodies. *D*: the cell number of ghrelin-immunopositive cells in Tg and non littermates. *E*: the mRNA levels of ghrelin in 12-wk-old male Tg mice and non littermates; $n = 5$, $^{**}P < 0.01$ compared with nontransgenic littermates. *F* and *G*: tissue concentration per milligram (*F*) and per stomach (*G*) of ghrelin peptide in 12-wk-old male Tg mice (black bars) and non littermates (open bars); $n = 6$, $^{**}P < 0.01$ compared with non littermates. C-RIA, total ghrelin (ghrelin and desacyl ghrelin); N-RIA, ghrelin. *H*: Western blot analysis of stomach samples of Tg and non littermates using anti COOH-terminal ghrelin antibody. *I*: RT-PCR analysis of prohormone convertase 1/3 (PC1/3) mRNA expression in the stomach of Tg.

modest even at 50 wk of age in the 4-3 line. Accordingly, we analyzed mainly GP-Tag Tg mice of the 3-1 line.

We could not get a transgene-positive mouse of GP (1479) Tag Tg mouse by injecting transgenes into 631 eggs.

The expression levels of SV40-Tag mRNA among various tissues. We first examined the expression levels of SV40-Tag mRNA in various tissues of GP-Tag Tg mice, including stomach, small intestine, colon, hypothalamus, pituitary, thyroid,

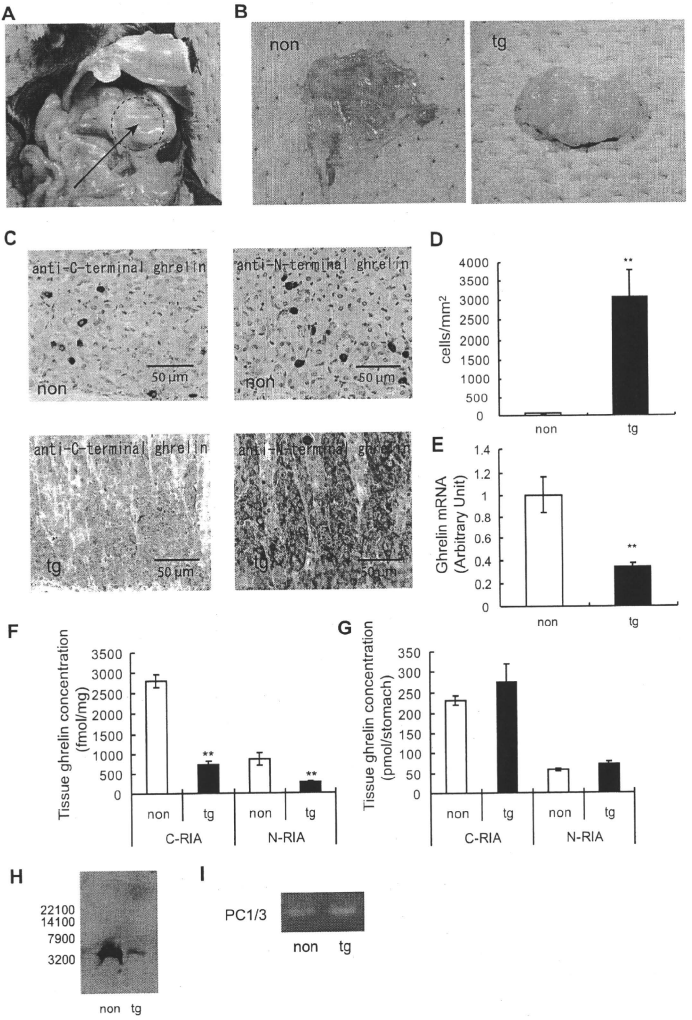

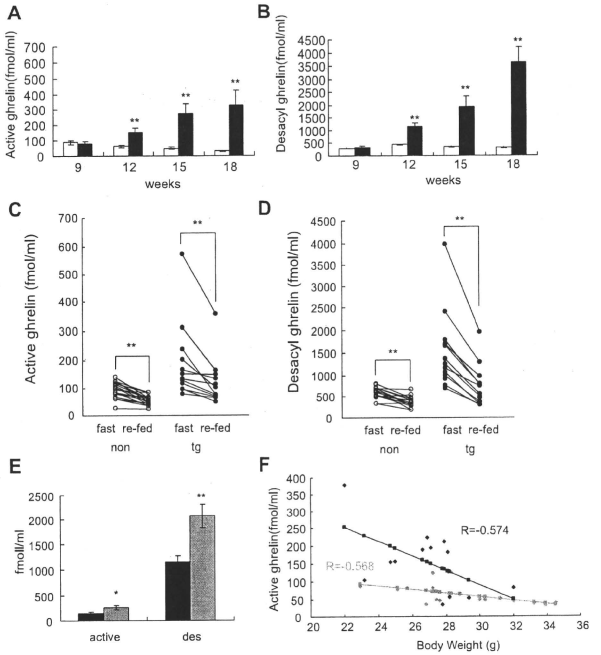

Fig. 3. Plasma ghrelin and desacyl ghrelin levels in GP-Tag Tg mice. *A* and *B*: plasma ghrelin (*A*) and desacyl ghrelin (*B*) levels in male GP-Tag Tg mice (black bars) and nontransgenic littermates (open bars); $n = 3$–17. $^{**}P < 0.01$ compared with non littermates. *C* and *D*: plasma ghrelin (*C*) and desacyl ghrelin (*D*) levels after overnight fasting (fast) and after refeeding (refed) in 15-wk-old male Tg and non mice. $^{**}P < 0.01$; $n = 12$–18. *E*: plasma ghrelin (active) and desacyl ghrelin (des) levels in 12-wk-old male (black bars) and female (gray bars) GP-Tag Tg mice; $n = 7$–13, $^{*}P < 0.05$, $^{**}P < 0.01$ compared with male GP-Tag Tg mice. *F*: plasma ghrelin levels were correlated with body weights in 12-wk-old male GP-Tag Tg mice (black bars; $r = -0.574$, $P < 0.01$) and in nontransgenic littermates (gray bars; $r = -0.568$, $P < 0.05$). The regression coefficient of the regression line of GP-Tag Tg mice was bigger than that of nontransgenic littermates ($t = 2.08$, $P < 0.05$).

pancreas, liver, heart, kidney, and testis (Fig. 1*B*). The highest expression levels were observed in stomach, and the second-highest levels were observed in small intestine. The expression pattern of SV40-Tag mRNA was almost similar to that of ghrelin (Fig. 1*C*).

Pathological feature and tissue ghrelin concentration of stomach of GP-Tag Tg mice. Stomach walls of GP-Tag Tg mice became hypertrophic with age (Fig. 2, *A* and *B*). Immunohistochemical analysis by both anti-COOH-terminal and anti-NH_2-terminal ghrelin antibodies revealed hyperplasia of ghrelin-immunopositive cells (Fig. 2, *C* and *D*), although the staining in GP-Tag Tg mice was paler than that in nontransgenic littermates (Fig. 2*C*). These hyperproliferating cells were not immunostained with anti-glucagon, somatostatin, or gastrin antibodies (data not shown).

The mRNA levels of ghrelin in the stomachs of 12-wk-old male GP-Tag Tg mice were significantly lower than those of nontransgenic littermates ($P < 0.01$, $n = 6$; Fig. 2*E*). Consistent with this observation, tissue concentrations of ghrelin (N-RIA; fmol/mg tissue) and total ghrelin (desacyl ghrelin plus ghrelin) (C-RIA) of 12-wk-old male GP-Tag Tg mice were significantly lower than those of nontransgenic littermates ($P < 0.01$, $n = 6$; Fig. 2*F*). However, since the weights of the stomach of GP-Tag Tg mice were significantly higher than controls (non-Tg vs. Tg, 83.4 vs. 362.0 mg, $P < 0.01$) due to the hypertrophy of the stomach wall, the tissue ghrelin concentration per whole stomach tended to be higher in GP-Tag Tg mice [not significant (NS), $n = 6$; Fig. 2*G*]. The size of ghrelin content of GP-Tag Tg mice was similar to that of nontransgenic littermates when analyzed by tricine-SDS PAGE and Western blot analysis (Fig. 2*H*), indicating that processing of preproghrelin to ghrelin occurred in hyperproliferaing ghrelin cells in GP-Tag Tg mice. The mRNA of prohormone convertase 1/3, which processes preproghrelin to ghrelin, was detected in the stomachs of GP-Tag Tg mice (Fig. 2*I*).

Plasma ghrelin levels of GP-Tag Tg mice. Plasma ghrelin and desacyl ghrelin levels of GP-Tag Tg mice were almost equal to those of nontransgenic littermates at 9 wk of age and then increased with age ($n = 3$–17; Fig. 3, *A* and *B*), with some variations in the levels among animals.

We next examined whether physiological regulation of ghrelin secretion is preserved in GP-Tag Tg mice. Plasma ghrelin and desacyl ghrelin levels of GP-Tag Tg mice were increased by fasting and decreased by refeeding $P < 0.01$, ($n = 7$–13; Fig. 3, *C* and *D*). Plasma ghrelin and desacyl ghrelin levels of female GP-Tag Tg mice were significantly higher than those of

male GP-Tag Tg mice at 12 wk of age (Fig. 3*E*). Plasma ghrelin levels of 12-wk-old male GP-Tag Tg mice correlated to body weight ($r = 0.574$, $P < 0.05$, $n = 13$; Fig. 3*F*). The regression coefficient of the regression line of GP-Tag Tg mice was bigger than that of nontransgenic littermates ($t = 2.08$, $P < 0.05$) These results indicate that regulation of plasma ghrelin and desacyl ghrelin levels of GP-Tag Tg mice were preserved, at least with regard to feeding status, body weight, and sex difference.

Body weights, body composition, and food intake of GP-Tag Tg mice. There was no difference in body weights between male GP-Tag Tg mice and controls until 12 wk of age ($n = 22$–34; Fig. 4*A*). After 13 wk of age, the body weights of the male GP-Tag Tg mice were significantly lower than those of nontransgenic littermates concomitantly with the decrease in the food intakes of male GP-Tag Tg mice after 11 wk of age (Fig. 4, *A* and *B*). When the body compositions were examined by computed tomography scan, fat masses were significantly reduced in 15-wk-old male GP-Tag Tg mice ($P < 0.05$, $n = 7$–9; Fig. 4*C*), whereas lean body masses and body lengths were not changed (NS, $n = 7$–9; Fig. 4, *D* and *E*). We also examined hypothalamic mRNA levels of neuropeptide Y (NPY), agouti-related protein (AgRP), and GHS-R in 12-wk-old male GP-Tag Tg mice. No significant changes were observed in these mRNA levels (NS, $n = 7$; Fig. 4*F*). When 15-wk-old male GP-Tag Tg mice were injected with ghrelin, the food intake was stimulated to the same extent as in controls (NS, $n = 10$–18; Fig. 4*G*). Plasma leptin levels of 15-wk-old male GP-Tag Tg mice were significantly lower than controls ($P < 0.05$, $n = 6$; Fig. 4*H*).

GH-IGF-I axis in GP-Tag Tg mice. Serum IGF-I levels of 12- and 15-wk-old male GP-Tag Tg mice were significantly higher than those of nontransgenic littermates ($P < 0.05$, $n = 7$–8, and $P < 0.05$, $n = 6$–7, respectively; Fig. 5*A*). Although basal serum GH levels of 15-wk-old male GP-Tag Tg mice were not significantly different from controls, serum GH levels after GHRH injection tended to be high ($P = 0.077$, $n = 8$–13), which was not observed after ghrelin injection (Fig. 5*B*). We then investigated the effects of chronic ghrelin elevation on hypothalamic and pituitary mRNA levels of components involved in GH regulation. There were no differences in hypothalamic mRNA levels of GHRH and somatostatin or in pituitary mRNA levels of GH and GHRH receptor (GHRH-R) between 15-wk-old male GP-Tag Tg mice and their littermates

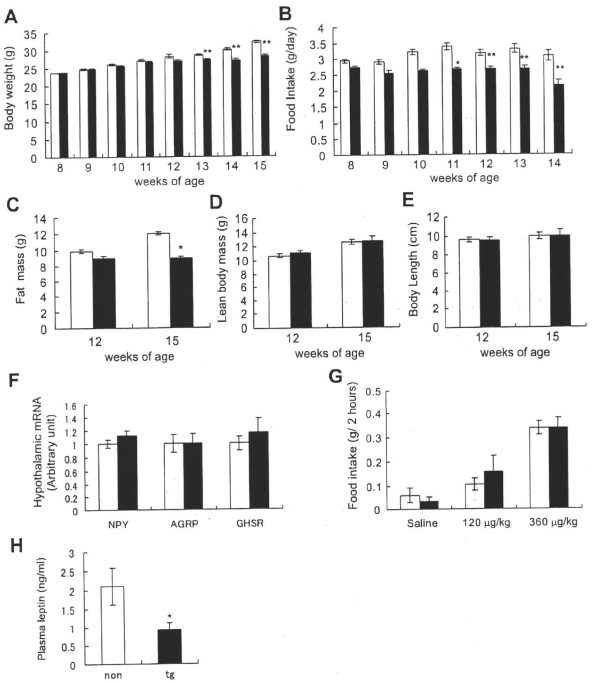

Fig. 4. Body weights, body compositions, and food intakes of GP-Tag Tg mice. *A*: body weights of male GP-Tag Tg mice (black bars) and nontransgenic littermates (open bars); $n = 22$–34. *B*: daily food intakes of male GP-Tag Tg mice (black bars) and nontransgenic littermates (open bars); $n = 19$–26. *C* and *D*: fat mass (*C*) and lean body mass (*D*) determined by animal computed tomography scan of 15-wk-old male GP-Tag Tg mice (black bars) and nontransgenic littermates (open bars). *E*: body length of 15-wk-old male GP-Tag Tg mice (black bars) and nontransgenic littermates (open bars); $n = 7$–9. *F*: hypothalamic mRNA levels of neuropeptide Y (NPY), agouti-related protein (AgRP), and growth hormone secretagogue receptor (GHS-R) in 12-wk-old male GP-Tag Tg mice (black bars) and nontransgenic littermates (open bars); $n = 7$. *G*: food intake for 2 h after injection of ghrelin (120 or 360 μg/kg or saline; $n = 10$–18). *H*: plasma leptin levels in 15-wk-old male Tg mice (black bars) and non littermates (open bars); $n = 6$–7. $^*P < 0.05$, $^{**}P < 0.01$ compared with nontransgenic littermates.

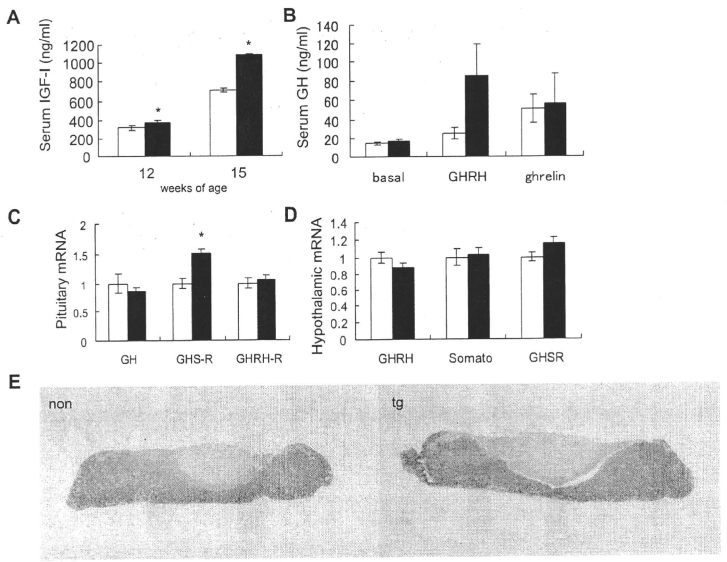

Fig. 5. GH-IGF-I axis in GP-Tag Tg mice. *A*: serum IGF-I levels in male GP-Tag Tg mice (black bars) and nontransgenic littermates (open bars); $n = 7–8$. *B*: serum GH levels at basal state and at 15 min after subcutaneous injection of GH-releasing hormone (GHRH) or ghrelin in male GP-Tag Tg mice (black bars) and nontransgenic littermates (open bars); $n = 8–13$. *C*: pituitary mRNA levels of GH, GHS-R, and GHRH-R in 15-wk-old male GP-Tag Tg mice (black bars) and nontransgenic littermates (open bars); $n = 7$. *D*: hypothalamic mRNA levels of GHRH, somatostatin (somato), and GHS-R in 15-wk-old male GP-Tag Tg mice (black bars) and nontransgenic littermates (open bars); $n = 7$. *E*: pituitary sections of 15-wk-old male Tg mice and non littermates immunostained with anti-GH antibody. $^*P < 0.05$ compared with non littermates.

(NS, $n = 7$; Fig. 5, *C* and *D*). Although plasma ghrelin level was elevated, pituitary GHS-R mRNA level was upregulated in GP-Tag Tg mice ($P < 0.05$, $n = 7$; Fig. 5*C*). We also examined pituitaries of 15-wk-old male GP-Tag Tg mice by immunohistochemical analysis. There were no obvious differences in somatotroph cell number or staining intensity of GH between GP-Tag Tg mice and nontransgenic littermates (Fig. 5*E*).

Glucose metabolism in GP-Tag Tg mice. Blood glucose levels of 15-wk-old male GP-Tag Tg mice were significantly higher than controls ($P < 0.05$, $n = 10$; Fig. 6*A*), although those of 9-wk-old male GP-Tag Tg mice were comparable with the controls (non-Tg vs. Tg: 96.0 ± 4.7 vs. 100.6 ± 4.7, $P = 0.51$, $n = 9$). Intraperitoneal glucose tolerance tests showed significantly higher blood glucose levels in 15-wk-old male GP-Tag Tg mice ($P < 0.05$, $n = 6–11$; Fig. 6*B*). To estimate the insulin sensitivity of GP-Tag Tg mice, we performed an insulin tolerance test. The blood glucose levels after insulin injection in 15-wk-old male GP-Tag Tg mice were suppressed to the same level of those in controls (NS, $n = 5–8$; Fig. 6*C*). Although basal insulin levels of 15-wk-old male GP-Tag Tg mice were not significantly different from those of control mice, those after glucose injection were significantly suppressed in GP-Tag Tg mice ($P < 0.05$, $n = 7–8$; Fig. 6*D*). Pancreatic mRNA and protein levels of insulin in GP-Tag Tg were comparable with those of nontransgenic littermates (NS, $n = 6–8$; Fig. 6, *E* and *F*).

DISCUSSION

In this study, we successfully established a mouse model of ghrelinoma, GP-Tag Tg mouse. GP-Tag Tg mice exhibited chronic elevation of circulating ghrelin with physiological regulation. The elevation of circulating ghrelin in GP-Tag Tg mice (~10-fold elevation) was much higher than that in bacterial artificial chromosome transgenic mice created by Bewick et al. (5) (only ~1.5-fold elevation). Nevertheless, the levels of circulating ghrelin in GP-Tag Tg mice can be considered to be within the physiological range since the highest level of plasma ghrelin observed in the anorexia patients is about seven times higher than those of normal controls (3). One may be confused by low ghrelin mRNA levels and low ghrelin production per milligram of tissue in the stomachs of GP-Tag Tg mice. In general, when the cell cycle progresses, endocrine cell produces far less amounts of hormone since the hormone production occurs mainly at the G_0/G_1 phase of the cell cycle. Since the hyperproliferaing ghrelin-producing cells in GP-Tag Tg mice were forced to proliferate by SV40 T-antigen, which suppresses RB protein and p53, promoting cell cycle progres-

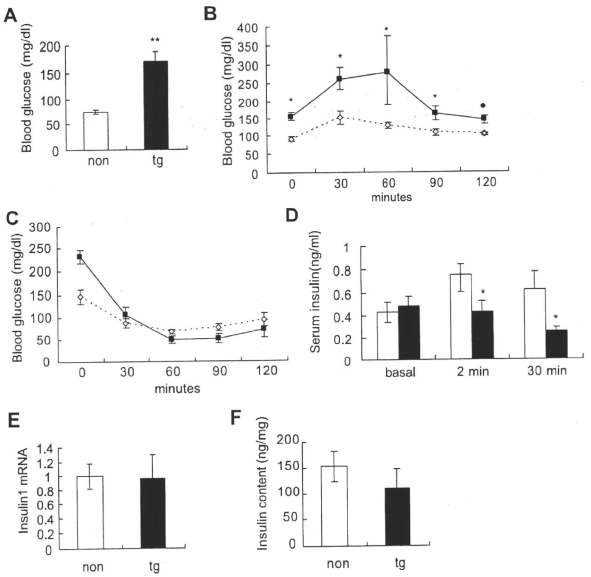

Fig. 6. Glucose metabolism in GP-Tag Tg mice. *A*: fasting blood glucose levels in 15-wk-old male Tg (black bar) and in non (open bar); $n = 7–10$. *B*: glucose tolerance tests in 15-wk-old male GP-Tag Tg mice (■) and in their nontransgenic littermates (◇); $n = 6–11$. *C*: insulin tolerance tests in male GP-Tag Tg mice (■) and in their nontransgenic littermates (◇); $n = 5–8$. *D*: serum insulin levels at basal, at 2 min, and at 30 min after intraperitoneal glucose injection in 15-wk-old male GP-Tag Tg mice (black bars) and in their nontransgenic littermates (open bars); $n = 7–8$. *E* and *F*: the mRNA (*E*) and the protein levels (*F*) of insulin in the pancreata of 15-wk-old male Tg mice (black bars) and in their non littermates (open bars); $n = 6–8$. $^*P < 0.05$, $^{**}P < 0.01$ compared with nontransgenic littermates.

sion, the amount of ghrelin production per cell was low. However, since the cell number was extremely increased, the net product by stomach was eventually elevated.

Several lines of evidence suggest that the GH-IGF-I axis is suppressed in the decreased GHS-R signaling state (28, 32). It has not yet been clear, however, whether chronic elevation of ghrelin within the physiological range could stimulate the GH-IGF-I axis. In this study, we found that adult GP-Tag Tg mice with elevated circulating ghrelin level showed elevated serum IGF-I level. Serum IGF-I level is regulated not only by GH but also by nutritional status. Malnutrition suppresses serum IGF-I level, whereas overnutrition elevates it (16). Since the nutritional state of GP-Tag Tg mice was poor because of decreased food intake, the elevated serum IGF-I levels in adult GP-Tag Tg mice are considered not to be due to overnutrition but to be due to activation of GH-IGF-I axis. Our findings indicate that chronic elevation of circulating ghrelin within the physiological range can activate the GH-IGF-I axis. As far as we know, this is the first report demonstrating that increased levels of circulating ghrelin within the physiological range can elevate serum IGF-I levels in rodent.

The GH-releasing action of ghrelin requires GHRH (11), and when coadministered, synergistic effects can be observed (13). Since GH responses to GHRH tended to be enhanced in adult GP-Tag Tg, the activation of the GH-IGF-I axis in GP-Tag Tg may be in part due to potentiation of the GH-releasing effect of GHRH. When the mRNA levels of components of GH regulation in pituitary and hypothalamus of GP-Tag Tg mice were investigated, an elevation of the pituitary GHS-R mRNA level was found. It is not clear whether this elevation of GHS-R mRNA in the pituitary contributes to the activated GH-IGF-I axis, since the GH response to ghrelin was not changed in GP-Tag Tg mice. At least these findings indicate that desensitization of GH secretion to ghrelin or downregulation of GHS-R did not occur by chronic elevation of circulating ghrelin in GP-Tag Tg mice.

Adult GP-Tag Tg mice exhibited high glucose level in the basal state and by the glucose tolerance test. Although insulin production was not decreased in the pancreata of GP-Tag Tg mice, insulin secretion after glucose load was significantly attenuated. Since the insulin sensitivity of GP-Tag Tg mice was not reduced, the glucose intorelance in GP-Tag Tg mice was due mainly to the decreased insulin secretion. Given that GP-Tag Tg mice have gastric tumors, there is a possibility that the glucose intorelance is due to the tumors. However, the glucose intolerance observed in malignancy is due mainly to insulin resistance (8, 15), which may be evoked by cytokines (22, 24, 27). Since the glucose intolerance of GP-Tag Tg mice was caused mainly by decreased insulin secretion, it seems not to be the case. It has been reported that acute injection of ghrelin induces suppression of insulin secretion in rodents and humans (6, 30). Our findings suggest that chronic elevation of circulating ghrelin within the physiological range leads to glucose intorelance by suppressing insulin secretion.

There have been several reports regarding ghrelin-producing tumors (9, 17, 36, 37). Most of the cases did not present

elevated plasma ghrelin levels except for a few cases. A malignant ghrelinoma case reported by Tsolakis et al. (36) showed elevated plasma ghrelin level. This patient maintained his weight despite progression of the tumor, a symptom that might be linked to the elevated ghrelin level. During the clinical course, he developed severe diabetes mellitus, which is consistent with the phenotype of GP-Tag Tg mice. GH and IGF-I levels were normal in this case. A pancreatic ghrelinoma case reported by Corbetta et al. (9) also showed normal GH and IGF-I levels despite elevated plasma ghrelin level. In contrast to these human ghrelinoma cases, GP-Tag Tg mice showed elevated IGF-I levels. The cause of the difference in the GH-IGF-I levels between our mice and these human ghrelinoma cases is unclear. Since the first case mentioned above was a malignant gastric ghrelinoma with liver metastasis, and the second case was of pancreatic origin, plasma ghrelin level might be elevated without any physiological regulation in these cases, although detailed plasma ghrelin level changes were not documented. Considering that the physiological regulation of ghrelin secretion was kept in GP-Tag Tg mice, the circadian rhythm may be needed for ghrelin to keep stimulating the GH-IGF-I axis. Indeed, several reports have shown that chronic treatment of ghrelin attenuates GH response both in vivo and in vitro (35, 39) and that in vitro treatment of pituitary with ghrelin results in decreased GHS-R mRNA levels (21). Further case studies will be required to reveal the relationship between plasma ghrelin levels and the GH-IGF-I axis in human ghrelinoma patients.

The limitation of this study is that the assessment of orexigenic action of ghrelin is difficult in this mouse model since stomach walls of GP-Tag Tg mice gradually become hypertrophic after 9 wk of age, which might affect the feeding behavior. Indeed, GP-Tag Tg mice exhibited decreased food intake and weight reduction despite the elevated plasma ghrelin levels. The hypothalamic mRNA levels of NPY and AgRP, which mediate the orexigenic action of ghrelin (7, 31), were not upregulated in GP-Tag Tg mice. There is a possibility that desensitization of GHS-R to chronic elevated ghrelin may be a cause of the lack of activation of these neurons besides the hypertrophy of the stomach wall. However, hypothalamic mRNA level of GHS-R was not changed. Furthermore, the food intake induced by acute ghrelin administration in GP-Tag Tg mice was comparable with control. These results may not support the idea of desensitization. Leptin and ghrelin have opposing effects on food intake. We examined whether plasma leptin levels of GP-Tag Tg mice were elevated as a compensation for the chronically elevated plasma ghrelin levels, which may cause anorexia. However, the leptin levels were decreased, provably reflecting the decreased fat mass of GP-Tag Tg mice.

In summary, we developed a mouse model of ghrelinoma, GP-Tag Tg mice, in which ghrelin concentrations were significantly elevated in adulthood. These GP-Tag Tg mice exhibited elevated IGF-I levels despite poor nutrition and glucose intolerance due to decreased insulin secretion. These characteristic features of this ghrelinoma mouse could be a guide to diagnose ghrelinoma.

ACKNOWLEDGMENTS

We thank Chieko Ishimoto and Chinami Shiraiwa for excellent technical assistance.

GRANTS

This study was supported by funds from the Ministry of Education, Culture, Sports, Science, and Technology of Japan and the Ministry of Health, Labour, and Welfare of Japan, a research grant from the Program for Promotion of Fundamental Studies in Health Sciences of the National Institute of Biomedical Innovation, and the Takeda Scientific Foundation in Japan.

REFERENCES

1. **Akamizu T, Shinomiya T, Irako T, Fukunaga M, Nakai Y, Kangawa K.** Separate measurement of plasma levels of acylated and desacyl ghrelin in healthy subjects using a new direct ELISA assay. *J Clin Endocrinol Metab* 90: 6–9, 2005.
2. **Ariyasu H, Takaya K, Iwakura H, Hosoda H, Akamizu T, Arai Y, Kangawa K, Nakao K.** Transgenic mice overexpressing des-acyl ghrelin show small phenotype. *Endocrinology* 146: 355–364, 2005.
3. **Ariyasu H, Takaya K, Tagami T, Ogawa Y, Hosoda K, Akamizu T, Suda M, Koh T, Natsui K, Toyooka S, Shirakami G, Usui T, Shimatsu A, Doi K, Hosoda H, Kojima M, Kangawa K, Nakao K.** Stomach is a major source of circulating ghrelin, and feeding state determines plasma ghrelin-like immunoreactivity levels in humans. *J Clin Endocrinol Metab* 86: 4753–4758, 2001.
4. **Asakawa A, Inui A, Fujimiya M, Sakamaki R, Shinfuku N, Ueta Y, Meguid MM, Kasuga M.** Stomach regulates energy balance via acylated ghrelin and desacyl ghrelin. *Gut* 54: 18–24, 2005.
5. **Bewick GA, Kent A, Campbell D, Patterson M, Ghatei MA, Bloom SR, Gardiner JV.** Mice with hyperghrelinemia are hyperphagic and glucose intolerant and have reduced leptin sensitivity. *Diabetes* 58: 840–846, 2009.
6. **Broglio F, Arvat E, Benso A, Gottero C, Muccioli G, Papotti M, van der Lely AJ, Deghenghi R, Ghigo E.** Ghrelin, a natural GH secretagogue produced by the stomach, induces hyperglycemia and reduces insulin secretion in humans. *J Clin Endocrinol Metab* 86: 5083–5086, 2001.
7. **Chen HY, Trumbauer ME, Chen AS, Weingarth DT, Adams JR, Frazier EG, Shen Z, Marsh DJ, Feighner SD, Guan XM, Ye Z, Nargund RP, Smith RG, Van der Ploeg LH, Howard AD, MacNeil DJ, Qian S.** Orexigenic action of peripheral ghrelin is mediated by neuropeptide Y and agouti-related protein. *Endocrinology* 145: 2607–2612, 2004.
8. **Copeland GP, Leinster SJ, Davis JC, Hipkin LJ.** Insulin resistance in patients with colorectal cancer. *Br J Surg* 74: 1031–1035, 1987.
9. **Corbetta S, Peracchi M, Cappiello V, Lania A, Lauri E, Vago L, Beck-Peccoz P, Spada A.** Circulating ghrelin levels in patients with pancreatic and gastrointestinal neuroendocrine tumors: identification of one pancreatic ghrelinoma. *J Clin Endocrinol Metab* 88: 3117–3120, 2003.
10. **Date Y, Kojima M, Hosoda H, Sawaguchi A, Mondal MS, Suganuma T, Matsukura S, Kangawa K, Nakazato M.** Ghrelin, a novel growth hormone-releasing acylated peptide, is synthesized in a distinct endocrine cell type in the gastrointestinal tracts of rats and humans. *Endocrinology* 141: 4255–4261, 2000.
11. **Dimaraki EV, Jaffe CA.** Role of endogenous ghrelin in growth hormone secretion, appetite regulation and metabolism. *Rev Endocr Metab Disord* 7: 237–249, 2006.
12. **Gutierrez JA, Solenberg PJ, Perkins DR, Willency JA, Knierman MD, Jin Z, Witcher DR, Luo S, Onyia JE, Hale JE.** Ghrelin octanoylation mediated by an orphan lipid transferase. *Proc Natl Acad Sci USA* 105: 6320–6325, 2008.
13. **Hataya Y, Akamizu T, Takaya K, Kanamoto N, Ariyasu H, Saijo M, Moriyama K, Shimatsu A, Kojima M, Kangawa K, Nakao K.** A low dose of ghrelin stimulates growth hormone (GH) release synergistically with GH-releasing hormone in humans. *J Clin Endocrinol Metab* 86: 4552, 2001.
14. **Hosoda H, Kojima M, Matsuo H, Kangawa K.** Ghrelin and des-acyl ghrelin: two major forms of rat ghrelin peptide in gastrointestinal tissue. *Biochem Biophys Res Commun* 279: 909–913, 2000.
15. **Isaksson B, Strommer L, Friess H, Buchler MW, Herrington MK, Wang F, Zierath JR, Wallberg-Henriksson H, Larsson J, Permert J.** Impaired insulin action on phosphatidylinositol 3-kinase activity and glucose transport in skeletal muscle of pancreatic cancer patients. *Pancreas* 26: 173–177, 2003.
16. **Iwakura H, Akamizu T, Ariyasu H, Irako T, Hosoda K, Nakao K, Kangawa K.** Effects of ghrelin administration on decreased growth hormone status in obese animals. *Am J Physiol Endocrinol Metab* 293: E819–E825, 2007.

17. **Iwakura H, Hosoda K, Doi R, Komoto I, Nishimura H, Son C, Fujikura J, Tomita T, Takaya K, Ogawa Y, Hayashi T, Inoue G, Akamizu T, Hosoda H, Kojima M, Kangawa K, Imamura M, Nakao K.** Ghrelin expression in islet cell tumors: augmented expression of ghrelin in a case of glucagonoma with multiple endocrine neoplasm type I. *J Clin Endocrinol Metab* 87: 4885–4888, 2002.
18. **Iwakura H, Hosoda K, Son C, Fujikura J, Tomita T, Noguchi M, Ariyasu H, Takaya K, Masuzaki H, Ogawa Y, Hayashi T, Inoue G, Akamizu T, Hosoda H, Kojima M, Itoh H, Toyokuni S, Kangawa K, Nakao K.** Analysis of rat insulin II promoter-ghrelin transgenic mice and rat glucagon promoter-ghrelin transgenic mice. *J Biol Chem* 280: 15247–15256, 2005.
19. **Kanamoto N, Akamizu T, Tagami T, Hataya Y, Moriyama K, Takaya K, Hosoda H, Kojima M, Kangawa K, Nakao K.** Genomic structure and characterization of the 5′-flanking region of the human ghrelin gene. *Endocrinology* 145: 4144–4153, 2004.
20. **Kojima M, Hosoda H, Date Y, Nakazato M, Matsuo H, Kangawa K.** Ghrelin is a growth-hormone-releasing acylated peptide from stomach. *Nature* 402: 656–660, 1999.
21. **Luque RM, Kineman RD, Park S, Peng XD, Gracia-Navarro F, Castano JP, Malagon MM.** Homologous and heterologous regulation of pituitary receptors for ghrelin and growth hormone-releasing hormone. *Endocrinology* 145: 3182–3189, 2004.
22. **Makino T, Noguchi Y, Yoshikawa T, Doi C, Nomura K.** Circulating interleukin 6 concentrations and insulin resistance in patients with cancer. *Br J Surg* 85: 1658–1662, 1998.
23. **Masuda Y, Tanaka T, Inomata N, Ohnuma N, Tanaka S, Itoh Z, Hosoda H, Kojima M, Kangawa K.** Ghrelin stimulates gastric acid secretion and motility in rats. *Biochem Biophys Res Commun* 276: 905–908, 2000.
24. **McCall JL, Tuckey JA, Parry BR.** Serum tumour necrosis factor alpha and insulin resistance in gastrointestinal cancer. *Br J Surg* 79: 1361–1363, 1992.
25. **Nagaya N, Kojima M, Uematsu M, Yamagishi M, Hosoda H, Oya H, Hayashi Y, Kangawa K.** Hemodynamic and hormonal effects of human ghrelin in healthy volunteers. *Am J Physiol Regul Integr Comp Physiol* 280: R1483–R1487, 2001.
26. **Nakazato M, Murakami N, Date Y, Kojima M, Matsuo H, Kangawa K, Matsukura S.** A role for ghrelin in the central regulation of feeding. *Nature* 409: 194–198, 2001.
27. **Noguchi Y, Yoshikawa T, Marat D, Doi C, Makino T, Fukuzawa K, Tsuburaya A, Satoh S, Ito T, Mitsuse S.** Insulin resistance in cancer patients is associated with enhanced tumor necrosis factor-alpha expression in skeletal muscle. *Biochem Biophys Res Commun* 253: 887–892, 1998.
28. **Pantel J, Legendre M, Cabrol S, Hilal L, Hajaji Y, Morisset S, Nivot S, Vie-Luton MP, Grouselle D, de Kerdanet M, Kadiri A, Epelbaum J, Le Bouc Y, Amselem S.** Loss of constitutive activity of the growth hormone secretagogue receptor in familial short stature. *J Clin Invest* 116: 760–768, 2006.
29. **Reed JA, Benoit SC, Pfluger PT, Tschöp MH, D'Alessio DA, Seeley RJ.** Mice with chronically increased circulating ghrelin develop age-related glucose intolerance. *Am J Physiol Endocrinol Metab* 294: E752–E760, 2008.
30. **Reimer MK, Pacini G, Ahren B.** Dose-dependent inhibition by ghrelin of insulin secretion in the mouse. *Endocrinology* 144: 916–921, 2003.
31. **Shintani M, Ogawa Y, Ebihara K, Aizawa-Abe M, Miyanaga F, Takaya K, Hayashi T, Inoue G, Hosoda K, Kojima M, Kangawa K, Nakao K.** Ghrelin, an endogenous growth hormone secretagogue, is a novel orexigenic peptide that antagonizes leptin action through the activation of hypothalamic neuropeptide Y/Y1 receptor pathway. *Diabetes* 50: 227–232, 2001.
32. **Shuto Y, Shibasaki T, Otagiri A, Kuriyama H, Ohata H, Tamura H, Kamegai J, Sugihara H, Oikawa S, Wakabayashi I.** Hypothalamic growth hormone secretagogue receptor regulates growth hormone secretion, feeding, and adiposity. *J Clin Invest* 109: 1429–1436, 2002.
33. **Tack J, Depoortere I, Bisschops R, Delporte C, Coulie B, Meulemans A, Janssens J, Peeters T.** Influence of ghrelin on interdigestive gastrointestinal motility in humans. *Gut* 55: 327–333, 2006.
34. **Takaya K, Ariyasu H, Kanamoto N, Iwakura H, Yoshimoto A, Harada M, Mori K, Komatsu Y, Usui T, Shimatsu A, Ogawa Y, Hosoda K, Akamizu T, Kojima M, Kangawa K, Nakao K.** Ghrelin strongly stimulates growth hormone release in humans. *J Clin Endocrinol Metab* 85: 4908–4911, 2000.
35. **Thompson NM, Davies JS, Mode A, Houston PA, Wells T.** Pattern-dependent suppression of growth hormone (GH) pulsatility by ghrelin and GH-releasing peptide-6 in moderately GH-deficient rats. *Endocrinology* 144: 4859–4867, 2003.
36. **Tsolakis AV, Portela-Gomes GM, Stridsberg M, Grimelius L, Sundin A, Eriksson BK, Oberg KE, Janson ET.** Malignant gastric ghrelinoma with hyperghrelinemia. *J Clin Endocrinol Metab* 89: 3739–3744, 2004.
37. **Volante M, Allia E, Gugliotta P, Funaro A, Broglio F, Deghenghi R, Muccioli G, Ghigo E, Papotti M.** Expression of ghrelin and of the GH secretagogue receptor by pancreatic islet cells and related endocrine tumors. *J Clin Endocrinol Metab* 87: 1300–1308, 2002.
38. **Wei W, Qi X, Reed J, Ceci J, Wang HQ, Wang G, Englander EW, Greeley GH Jr.** Effect of chronic hyperghrelinemia on ingestive action of ghrelin. *Am J Physiol Regul Integr Comp Physiol* 290: R803–R808, 2006.
39. **Yamazaki M, Nakamura K, Kobayashi H, Matsubara M, Hayashi Y, Kangawa K, Sakai T.** Regulational effect of ghrelin on growth hormone secretion from perifused rat anterior pituitary cells. *J Neuroendocrinol* 14: 156–162, 2002.
40. **Yang J, Brown MS, Liang G, Grishin NV, Goldstein JL.** Identification of the acyltransferase that octanoylates ghrelin, an appetite-stimulating peptide hormone. *Cell* 132: 387–396, 2008.
41. **Zhang W, Chai B, Li JY, Wang H, Mulholland MW.** Effect of des-acyl ghrelin on adiposity and glucose metabolism. *Endocrinology* 149: 4710–4716, 2008.

FEBS Letters 583 (2009) 1029–1033

FEBS Letters

journal homepage: www.FEBSLetters.org

Adipogenic differentiation of human induced pluripotent stem cells: Comparison with that of human embryonic stem cells

Daisuke Taura [a,1], Michio Noguchi [a,1], Masakatsu Sone [a,*], Kiminori Hosoda [a,*], Eisaku Mori [a], Yohei Okada [b], Kazutoshi Takahashi [c,d], Koichiro Homma [a,e], Naofumi Oyamada [a], Megumi Inuzuka [a], Takuhiro Sonoyama [a], Ken Ebihara [a], Naohisa Tamura [a], Hiroshi Itoh [e], Hirofumi Suemori [f], Norio Nakatsuji [g,h], Hideyuki Okano [b], Shinya Yamanaka [c,d], Kazuwa Nakao [a]

[a] Department of Medicine and Clinical Science, Kyoto University Graduate School of Medicine, 54 Shogoin Kawahara-cho, Sakyo-ku, Kyoto 606-8507, Japan
[b] Department of Physiology, Keio University, School of Medicine, Tokyo, Japan
[c] Department of Stem Cell Biology, Institute for Frontier Medical Sciences, Kyoto University, Kyoto, Japan
[d] Center for iPS Cell Research and Application (CiRA), Institute for Integrated Cell-Material Sciences, Kyoto, Japan
[e] Department of Internal Medicine, Keio University School of Medicine, Tokyo, Japan
[f] Laboratory of Embryonic Stem Cell Research, Stem Cell Research Center, Institute for Frontier Medical Sciences, Kyoto University, Kyoto, Japan
[g] Department of Development and Differentiation, Institute for Frontier Medical Sciences, Kyoto University, Kyoto, Japan
[h] Institute for Integrated Cell-Material Sciences (iCeMS), Kyoto University, Kyoto, Japan

ARTICLE INFO

Article history:
Received 28 December 2008
Revised 10 February 2009
Accepted 21 February 2009
Available online 27 February 2009

Edited by Robert Barouki

Keywords:
Adipogenesis
Adipocyte
Stem cell
Differentiation

ABSTRACT

Induced pluripotent stem (iPS) cells were recently established from human fibroblasts. In the present study we investigated the adipogenic differentiation properties of four human iPS cell lines and compared them with those of two human embryonic stem (ES) cell lines. After 12 days of embryoid body formation and an additional 10 days of differentiation on Poly-L-ornithine and fibronectin-coated dishes with adipogenic differentiation medium, human iPS cells exhibited lipid accumulation and transcription of adipogenesis-related molecules such as C/EBPα, PPARγ2, leptin and aP2. These results demonstrate that human iPS cells have an adipogenic potential comparable to human ES cells.

1. Introduction

Pluripotent embryonic stem (ES) cells have been considered potent candidates for regenerative medicine as an unlimited source of cells for the transplantation therapy and a useful tool for the investigation of cell development/differentiation, especially after establishment of human ES cells [1]. We previously clarified the differentiation process of mouse, monkey and human ES cells into vascular cells [2–4] and demonstrated that transplantation of vascular cells derived from human ES cells may constitute a novel strategy for vascular regeneration [4,5]. A number of immunological and ethical problems remain to be overcome before clinical application of the ES cells, however. Recently, novel ES cell-like pluripotent cells, termed induced pluripotent stem (iPS) cells, were generated by introducing four transcription factors (Oct3/4, Sox2, Klf4 and c-Myc) into mouse skin fibroblasts [6], and soon thereafter iPS cells were also generated from human skin fibroblasts [7,8]. Since then, a new generation of human iPS cells has been generated by introducing into fibroblasts just three of the aforementioned transcription factors (c-Myc was omitted) [9]. By overcoming the immunological and ethical problems associated with ES cells, iPS cells open a new avenue for cell transplantation-based regenerative medicine and provide a powerful new tool with which to investigate organ development/differentiation in specific disease states, especially in inherited diseases.

Generalized lipodystrophy consists of congenital and acquired types characterized by the lack of the whole adipose tissue, which leads to severe insulin-resistant diabetes, hypertriglyceridemia and fatty liver. We previously analyzed genes and phenotypes of congenital generalized lipodystrophic Japanese [10] and also demonstrated the long-lasting efficacy and safety of the leptin-replacement therapy in these patients [11–13]. Since metabolic abnormality in the mouse model is known to be cured by mature

* Corresponding authors. Fax: +81 75 771 9452.
E-mail addresses: sonemasa@kuhp.kyoto-u.ac.jp (M. Sone), kh@kuhp.kyoto-u.ac.jp (K. Hosoda).
[1] These authors contributed equally to this work.

0014-5793/$36.00
doi:10.1016/j.febslet.2009.02.031

adipocytes transplantation, the regeneration therapy of the adipose tissue with human iPS cells-derived adipocytes is the ideal goal for lipodystrophic patients. Moreover, in vitro adipogenic differentiation system of human iPS cells will contribute to elucidate the pathogenesis of congenital generalized lipodystrophy when iPS cell lines are established from patients with lipodystrophy. In the present study we have investigated the adipogenic differentiation of human iPS cells and compared with that of human ES cells.

2. Materials and methods

2.1. Cells and culture

Four human iPS cell lines (201B6, 201B7, 253G1 and 253G4) were investigated. The 201B6 (B6) and 201B7 (B7) lines were generated by introducing four transcription factors (Oct3/4, Sox2, Klf4 and c-Myc) into human skin fibroblasts while the 253G1 (G1) and 253G4 (G4) lines were generated using only three factors (c-Myc was omitted) [9]. These iPS cell lines were maintained as previously described [7]. Two human ES cell lines (H9 and KhES-1) were used and maintained as previously described [1,14].

2.2. Adipogenic differentiation

For embryoid body (EB) formation, iPS and ES colonies were digested with 1 mg/ml collagenase type IV (GIBCO, CA, USA) and plated onto non-adherent bacterial culture dishes, where they were allowed to aggregate in maintenance medium without bFGF. Retinoic acid (Sigma–Aldrich, Japan) was added to the medium to a concentration of 100 nM from day 2 to day 5. After 12 days, EBs were transferred to 6-well plates coated with a combination of 30 μg/ml Poly-L-ornithine (Sigma–Aldrich) and 2 μg/ml fibronectin (Sigma–Aldrich). To induce adipocyte differentiation from iPS and ES cells, we applied a modification of a procedure described previously for use with mouse and human ES cells (Fig. 1) [15–19]. Differentiation was induced for 10 days using medium consisting of DMEM-F12, 10% KSR, and an adipogenic cocktail (0.5 mM IBMX, 0.25 μM dexamethasone, 1 μg/ml insulin, 0.2 mM indomethacin and 1 μM pioglitazone).

2.3. Immunocytochemistry

Immunocytochemistry was carried out as previously described [7]. The anti-human primary antibodies included Nanog (R&D Systems, MN, USA) and Alexa 488-conjugated SSEA-4 (Santa Cruz Biotechnology Inc., CA, USA) and TRA1-60 (CHEMICON, LA, USA). The TRA1-60 antibody was labeled using an Alexa Fluor 488 Monoclonal Antibody Labeling Kit (Molecular Probes, OR, USA). Alexa 546-conjugated donkey anti-sheep IgG (Molecular Probes, OR, USA) served as the secondary antibody. Alkaline phosphatase activity was detected using a BCIP/NBT substrate system (Dakocytomation, CA, USA).

2.4. Oil Red O staining and microscopic analysis of adipocytes

Cells were washed with phosphate-buffered saline (PBS) twice, fixed in 3.7% formaldehyde for 1 h and then stained with 0.6% (w/v) Oil Red O (Nacalai Tesque, Japan) solution (60% isopropanol, 40% water) for 2 h at room temperature. The cells were then washed with water to remove unbound dye. Subsequently, the bound Oil Red O was eluted with isopropanol.

Table 1
Primers for reverse-transcription polymerase chain reaction.

Gene		Sequence
Nanog	Sense	CAGCCCCGATTCTTCCACCAGTCCC
	Antisense	CGGAAGATTCCCAGTCGGGTTCACC
PPARγ2	Sense	ATTGACCCAGAAAGCGATTC
	Antisense	CAAAGGAGTGGGAGTGGTCT
C/EBPα	Sense	GCAAACTCACCGCTCCAATG
	Antisense	TTAGGTTCCAAGCCCCAAGTC
aP2	Sense	AACCTTAGATGGGGGTGTCCTG
	Antisense	TCGTGGAAGTGACGCCTTTC
Leptin	Sense	GAACCCTGTGCGGATTCTTGTG
	Antisense	CGTTTCTTFAAGGCATACTGGTGAG
GAPDH	Sense	ACCACAGTCCATGCCATCAC
	Antisense	TCCACCACCCTGTTGCTGT
PPARγ2 (real-time RT-PCR)	Sense	GATACACTGTCTGCAAACATATCACAA
	Antisense	CCACGGAGCTGATCCCAA
	Probe	AGAGATGCCATTCTGGCCCACCAACTT

After staining with Oil Red O, each EB was examined microscopically for the presence of adipocyte colonies, and the percentage of EBs with outgrowths showing adipocyte positivity was determined as previously described [15]. EBs in which adipocytes accounted for more than half of their circumference were considered adipocyte-positive. The percent area of Oil Red O staining (+) was determined at 20× magnification by counting the number of pixels exhibiting Oil Red O positivity in selected microscope fields (449 × 338 pixels). Four randomly selected fields were examined in each well of a 6-well plate, and the percent area was calculated as the average for the four fields. Six independent experiments were performed for each cell line.

2.5. Reverse-transcription polymerase chain reaction (RT-PCR) and quantitative real-time PCR

Total RNA was extracted using TRizol Reagent (Invitrogen, CA, USA) and treated with RNase-Free DNase Set (QIAGEN, Germany) to remove any contaminating genomic DNA. For RT-PCR, cDNA was synthesized using a PrimeScript RT reagent Kit (Takara Bio Inc., Japan), after which RT-PCR was run using ExTaq (Takara Bio Inc.). For quantitative real-time PCR, TaqMan PCR was carried out using a Step One Plus Real-Time PCR System as instructed by the manufacturer (Applied Biosystems, CA, USA). Levels of mRNA were normalized to those of 18S mRNA. The primers used are listed in Table 1.

2.6. Statistical analysis

Data are expressed as means ± S.E.M. Statistical significance was evaluated using ANOVA for comparison among six groups. Values of $P < 0.05$ were considered significant.

3. Results

3.1. Adipogenic differentiation of human iPS and ES cells

Morphological phenotypes, immunoreactivities of Nanog, SSEA-4 and TRA-1-60, and ALP activity of human iPS cells did not differ

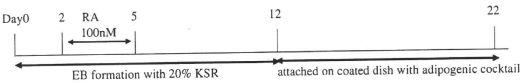

Fig. 1. Schematic diagram of the experimental protocol used for adipocyte differentiation from human ES and human iPS cells. EB: embryoid body. Adipogenic cocktail: 0.5 mM IBMX, 0.25 μM dexamethasone, 1 μg/ml insulin, 0.2 mM indomethacin and 1 μM pioglitazone.

from those of human ES cells (Fig. 2). In order to assess their potential for adipogenic differentiation, the human iPS cells were subjected to adipogenic induction culture. After 12 days of EB formation, EBs derived from human iPS cells were attached to coated dishes to induce differentiation. Several kinds of coating for the dishes, including gelatin, collagen IV and fibronectin were compared, and the efficiency of EB attachment and adipogenic differentiation were the best on dishes coated with a combination of Poly-L-ornithine and fibronectin. On day 15, after 3 days of adipogenic differentiation following the EB formation, differentiated cells containing small cytoplasmic lipid droplets were observed spreading outward from the attached EBs. On day 22, the lipid accumulation was evaluated by staining the cells with Oil Red O.

To evaluate the adipogenic potential of individual iPS cell lines, the percentage of EB outgrowths having adipocyte colonies and the percent area of Oil Red O staining (+) were determined. For each of iPS and ES cell lines tested, 40–60% of EBs formed adipocyte colonies (Table 2). In all of the iPS cell lines, lipid accumulation was similar to that seen in human ES cell lines (Fig. 3), though the B7 line showed stronger lipid accumulation than the other cell lines.

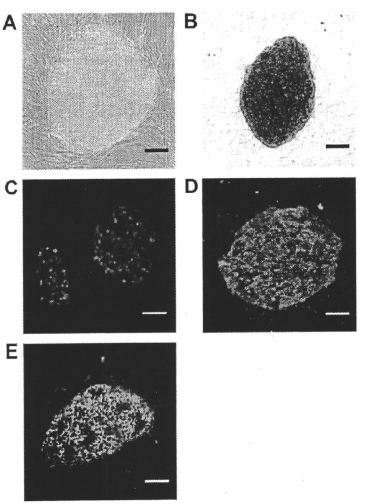

Fig. 2. Morphology of undifferentiated human iPS cells (G4). (A) Phase-contrast photomicrograph of an undifferentiated colony. (B) Alkaline phosphatase activity. (C) Immunofluorescent staining with Nanog. (D) Immunofluorescent staining with SSEA-4. (E) Immunofluorescent staining with TRA1-60. Scale bar = 100 μM.

Table 2
% of EBs with adipocyte colonies.

Cell line	[Number of EBs with adipocytecolonies/total number of EBs]
201B6	54.1% [40/74]
201B7	59.7% [46/77]
253G1	50.0% [35/70]
253G4	56.4% [44/78]
H9	48.8% [39/80]
KhES-1	45.5% [35/77]

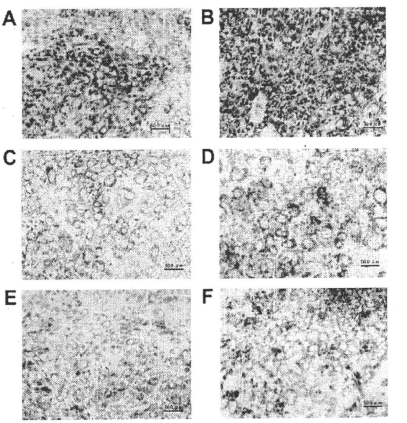

Fig. 3. Oil Red O staining of adipocytes derived from human iPS cells (A–D) and ES cells (E, F) on day 22. B6 (B) B7 (C) G1 (D) G4 (E) H9 (F) KhES-1. Scale bar = 50 μM.

Statistical analysis of the percent area of Oil Red O staining (+) showed no significant differences among the cell lines (Fig. 4).

3.2. Expression of adipogenesis-related molecules

Using RT-PCR, transcription of adipogenic markers was investigated on days 0 and 22 of differentiation (Fig. 5A). Though not detected at day 0, mRNAs encoding the adipogenic transcription factors C/EBPα (CCAAT/enhancer binding protein α) and PPARγ2 (peroxisome proliferator-activated receptor γ2) were detected on day 22. In contrast, expression of Nanog mRNA was strongly suppressed on day 22, as compared with its expression on day 0. Expression of the mature adipocyte markers leptin and aP2 (adipocyte fatty acid binding protein) was also clearly detected on day 22. All of the human iPS cell lines expressed mRNAs encoding adipogenesis-related molecules at levels that were comparable to the levels seen in human ES cell lines (Fig. 5A). In Quantitative real-time PCR analysis, expression of PPARγ2 mRNA differed somewhat among the iPS and ES cell lines. The differences between the B7 line and the two ES cell lines were significant, but other differences were not significant (Fig. 5B).

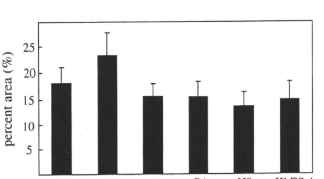

Fig. 4. Percent area of Oil Red O staining. Results are means of six independent experiments. No significant differences were observed among the iPS and ES cell lines.

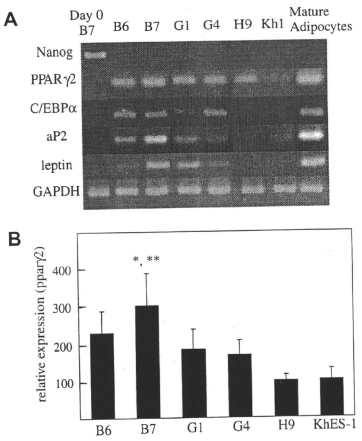

Fig. 5. (A) Transcription of the adipocyte-specific markers PPARγ2, CEBP/α, aP2 and leptin. RNA samples from undifferentiated human iPS cells (B7, day 0) and differentiated stage iPS cells (B6, B7, G1, G4) and human ES cells (H9, KhES-1), as well as mature human adipocytes differentiated from human adipose-derived mesenchymal stem cells (positive control), were analyzed by RT-PCR. Nanog is an undifferentiated human ES cell marker. GAPDH served as an internal standard for RT-PCR. Kh1: KhES-1. Adipose: human mature adipocytes differentiated from human adipose-derived mesenchymal stem cells. (B) Relative levels of PPARγ2 mRNA expression are shown as means ± S.E.M. of 4–6 independent experiments and normalized to those of 18S. The levels are expressed as percentages of the expression in the H9 cell line. *$P < 0.05$ vs. H9. **$P < 0.05$ vs. KhES-1.

4. Discussion

The present study demonstrates that human iPS cells have adipogenic potential comparable to human ES cells. Four human iPS cell lines of two generations were investigated. The B6 and B7 were generated by introducing four transcription factors (Oct3/4, Sox2, Klf4 and c-Myc) into human skin fibroblasts while the G1 and G4 were generated using only three factors (c-Myc was omitted) [9]. After 12 days of embryoid body formation and an additional 10 days of differentiation on Poly-L-ornithine and fibronectin-coated dishes with adipogenic differentiation medium, all human iPS cell lines of both generations exhibited lipid accumulation and transcription of such adipogenesis-related molecules as C/EBPα, PPARγ2, leptin and aP2. We also compared differentiation efficiency between human iPS and ES cells using two lines of human ES cells and found no apparent difference between human iPS and ES cells in properties of adipogenic differentiation including the time course and potential. In terms of lipid accumulation and transcription of adipogenesis-related molecules, human iPS-derived adipocytes appear to reach at least the same level of maturity as those derived from human ES cells. The B7 line tended to show stronger adipogenic potential than the other five iPS lines and the ES cell lines, but the difference in terms of percent area of Oil Red O staining (+) was not significant. The B7 line also showed significantly stronger expression of PPARγ2 than the two ES cell lines tested, but PPARγ2 expression varied among the different iPS cell lines, despite their having the same genetic background. We conclude that the adipogenic potential of iPS cells did not essentially differ from ES cells, though their adipogenic potentials were rather varied in each line.

Despite the prevalence of obesity, systems for research into human adipocyte biology remain underdeveloped, in part because of a lack of available human adipocyte cell lines. There are significant differences between adipocyte development in humans and mice [20]. The established in vitro adipocyte differentiation system using human iPS cells in the present study should make it possible to dissect out the cellular mechanisms underlying human adipocyte differentiation. It should also contribute to the better understanding of adipocyte biology and serve as a basis for advances in research into obesity and adipotoxicity, which has been proposed as the sum of the negative effects associated with obesity [21].

Adipogenesis is largely divided into two phases: the early phase consisting of the lineage commitment of adipocytes from pluripotent stem cells and the late phase consisting of the terminal differentiation of preadipocytes into adipocytes [22]. The molecular mechanism underlying the terminal adipocyte differentiation has been identified through analysis of the differentiation process in immortalized mouse preadipocyte cell lines (e.g., 3T3-L1 and 3T3-F442A cells) [22–24], but the differentiation from pluripotent stem cells during the early stage of adipogenesis must await further clarification. The establishment of adipocyte differentiation system with human iPS cells should facilitate that line of research.

In contrast to human ES cells, iPS cells can be induced from any human being irrespective of their genetic make-up. Consequently, the study of iPS cells should contribute to the identification of new susceptibility genes associated with obesity and metabolic syndrome, and to the clarification of the functions of those genes. The establishment of iPS cell lines from patients with inherited diseases presenting adipocyte abnormality should enable clarification of their pathogenesis. And because they overcome the immunological and ethical problems associated with human ES cells, iPS cell systems should also contribute to the development of novel regenerative therapies for reconstruction of soft tissue defects after tumor resections, extensive deep burns and lipodystrophy. The induced cells obtained with our protocol are not a homogeneous population. Consequently, at this stage human iPS cells may not yet have as much adipogenic potential as adipose-derived stem cells (ADSCs), which are derived from the stromal vascular fraction of human adipose tissue and are thought to be a safe and useful tool in adipose regenerative medicine [25]. About 80% of ADSCs differentiate into adipocytes under suitable conditions [26]. The next issue we plan to address will be the establishment of an improved differentiation protocol that includes a purification process such as cell sorting.

In conclusion, the present study demonstrates that human iPS cells have adipogenic potential that is generally equal to that of human ES cells. The use of iPS cells will contribute to the development of regenerative therapies of adipose tissue for lipodystrophy. This work should also contribute to our understanding of human adipogenesis and to the clarification of the pathogenesis and pathophysiology of obesity and metabolic syndrome, potentially leading to the development of new drug therapies.

Acknowledgement

We thank Yoshie Fukuchi for her technical assistance. This work was supported by the project for realization of regenerative medicine of the Ministry of Education, Culture, Sports, Science and Technology, Japan.

References

[1] Thomson, J.A., Itskovitz-Eldor, J., Shapiro, S.S., Waknitz, M.A., Swiergiel, J.J., Marshall, V.S. and Jones, J.M. (1998) Embryonic stem cell lines derived from human blastocytsts. Science 282, 1145–1147.

[2] Yamashita, J., Itoh, H., Hirashima, M., Ogawa, M., Nishikawa, S., Yurugi, T., Naito, M., Nakao, K., Nishikawa, S., et al. (2000) Flk1-positive cells derived from embryonic stem cells serve as vascular progenitors. Nature 408, 92–96.
[3] Sone, M., Itoh, H., Yamashita, J., Nakao, K., et al. (2003) Different differentiation kinetics of vascular progenitor cells in primate and mouse embryonic stem cells. Circulation 107, 2085–2088.
[4] Sone, M., Itoh, H., Nakao, K., et al. (2007) Pathway for differentiation of human embryonic stem cells to vascular cell components and their potential for vascular regeneration. Arterioscler. Thromb. Vasc. Biol. 27, 2127–2134.
[5] Yamahara, K., Sone, M., Itoh, H., Nakao, K., et al. (2008) Augmentation of Neovascularizaition in hindlimb ischemia by combined transplantation of human embryonic stem cells-derived endothelial and mural cells. PLOS One 3 (2), e1666.
[6] Takahashi, K. and Yamanaka, S. (2006) Induction of pluripotent stem cells from mouse embryonic and adult fibroblast cultures by defined factors. Cell 126, 663–676.
[7] Takahashi, K., Tanabe, K., Ohnuki, M., Narita, M., Ichisaka, T., Tomoda, K. and Yamanaka, S. (2007) Induction of pluripotent stem cells from adult human fibroblasts by defined factors. Cell 131, 861–872.
[8] Yu, J., Vodyanik, M.A., Smuga-Otto, K., Antosiewicz-Bourget, J., Frane, J.L., Tian, S., Nie, J., Jonsdottir, G.A., Ruotti, V., Stewart, R., Slukvin II and Thomson, J.A. (2007) Induced pluripotent stem cell lines derived from human somatic cells. Science 318, 1917–1920.
[9] Nakagawa, M., Koyanagi, M., Tanabe, K., Takahashi, K., Ichisaka, T., Aoi, T., Okita, K., Mochiduki, Y., Takizawa, N. and Yamanaka, S. (2008) Generation of induced pluripotent stem cells without Myc from mouse and human fibroblasts. Nat. Biotechnol. 26, 101–106.
[10] Ebihara, K., Kusakabe, T., Masuzaki, H., Kobayashi, N., Tanaka, T., Chusho, H., Miyanaga, F., Miyazawa, T., Hayashi, T., Hosoda, K., Ogawa, Y. and Nakao, K. (2004) Gene and phenotype analysis of congenital generalized lipodystrophy in Japanese: a novel homozygous nonsense mutation in seipin gene. J. Clin. Endocrinol. Metab. 89 (5), 2360–2364.
[11] Ebihara, K., Masuzaki, H. and Nakao, K. (2004) Long-term leptin-replacement therapy for lipoatrophic diabetes. New Engl. J. Med. 351 (6), 615–616.
[12] Ebihara, K., Kusakabe, T., Hirata, M., Masuzaki, H., Miyanaga, F., Kobayashi, N., Tanaka, T., Chusho, H., Miyazawa, T., Hayashi, T., Hosoda, K., Ogawa, Y., DePaoli, AM., Fukushima, M. and Nakao, K. (2007) Efficacy and safety of leptin-replacement therapy and possible mechanisms of leptin actions in patients with generalized lipodystrophy. J. Clin. Endocrinol. Metab. 92 (2), 532–541.
[13] Ebihara, K., Ogawa, Y., Masuzaki, H., Shintani, M., Miyanaga, F., Aizawa-Abe, M., Hayashi, T., Hosoda, K., Inoue, G., Yoshimasa, Y., Gavrilova, O., Reitman, ML. and Nakao, K. (2001) Transgenic overexpression of leptin rescues insulin resistance and diabetes in a mouse model of lipoatrophic diabetes. Diabetes 50 (6), 1440–1448.
[14] Fujioka, T., Yasuchika, K., Nakamura, Y., Nakatsuji, N. and Suemori, H. (2004) A simple and efficient cryopreservation method for primate embryonic stem cells. Int. J. Dev. Biol. 48, 1149–1154.
[15] Dani, C., Smith, A.G., Ailhaud, G., et al. (1997) Differentiation of embryonic stem cells into adipocytes in vitro. J. Cell. Sci. 110, 1279–1285.
[16] Xiong, C., Xie, C.Q., Chen, Y.E., et al. (2005) Derivation of adipocytes from human embryonic stem cells. Stem Cells Dev. 14, 671–675.
[17] van Harmelen, V., Astrom, G., Ryden, M., et al. (2007) Differential lipolytic regulation in human embryonic stem cell-derived adipocytes. Obesity 15, 846–852.
[18] Barberi, T., Willis, L.M., Socci, N.D. and Studer, L. (2005) Derivation of multipotent mesenchymal precursors from human embryonic stem cells. PLoS Med. 2, e161.
[19] Olivier, E.N., Rybicki, A.C. and Bouhassira, E.E. (2006) Differentiation of human embryonic stem cells into bipotent mesenchymal stem cells. Stem cells 24, 1914–1922.
[20] Arner, P. (2005) Resistin: yet another adipokine tells us that men are not mice. Diabetologia 48, 2203–2205.
[21] Nakao, K. (2009) Adiposcience and adipotoxicity. Nat. Clin. Pract. Endocrinol. Metab. 5 (2), 63.
[22] Rosen, E.D. and Spiegelman, B.M. (2000) Molecular regulation of adipogenesis. Annu. Rev. Cell. Dev. Biol. 16, 145–171.
[23] Bernlohr, D.A., Bolanowski, M.A., Kelly Jr., T.J. and Lane, M.D. (1985) Evidence for an increase in transcription of specific mRNAs during differentiation of 3T3-L1 preadipocytes. J. Biol. Chem. 260, 5563–5567.
[24] Flier, J.S. (2004) Obesity wars: molecular progress confronts an expanding epidemic. Cell 116, 337–350.
[25] Zuk, P.A., Zhu, M., Mizuno, H., Huang, J., Futrell, J.W., et al. (2001) Multilineage cells from human adipose tissue: Implications for cell-based therapies. Tissue Eng. 7, 211–228.
[26] Zhu, Y., Liu, T., Song, K., Fan, X., Ma, X. and Cui, Z. (2008) Adipose-derived stem cell: a better stem cell than BMSC. Cell Biochem. Funct. 26, 664–675.